Composite Structures 119 (2015) 67–89

Contents lists available at ScienceDirect

Composite Structures

journal homepage: www.elsevier.com/locate/compstruct

Stress and strain recovery for functionally graded free-form and doubly-curved sandwich shells using higher-order equivalent single layer theory

Francesco Tornabene [a,*,1], Nicholas Fantuzzi [a,1], Erasmo Viola [a,1], Romesh C. Batra [b]

[a] DICAM – Department, School of Engineering and Architecture, University of Bologna, Italy

[b] Department of Engineering Science and Mechanics, Virginia Polytechnic Institute and State University, M/C 0219, Blacksburg, VA 24061, USA

ARTICLE INFO

Article history:
Available online 23 August 2014

Keywords:
Functionally Graded Materials
Stress and strain recovery
Higher-order Shear Deformation Theory
Bézier curve
Generalized Differential Quadrature method

ABSTRACT

We investigate recovery of through-the-thickness transverse normal and shear strains and stresses in statically deformed functionally graded (FG) doubly-curved sandwich shell structures and shells of revolution using the generalized zigzag displacement field and the Carrera Unified Formulation (CUF). Three different through-the-thickness distributions of the volume fractions of constituents and two different homogenization techniques are employed to deduce the effective moduli of linear elastic isotropic materials. The system of partial differential equations for different Higher-order Shear Deformation Theories (HSDTs) is numerically solved by using the Generalized Differential Quadrature (GDQ) method. Either the face sheets or the core is assumed to be made of a FGM. The through-the-thickness stress profiles are recovered by integrating along the thickness direction the 3-dimensional (3-D) equilibrium equations written in terms of stresses. The stresses are used to find the strains by using Hooke's law. The computed displacements and the recovered through-the-thickness stresses and strains are found to compare well with those obtained by analyzing the corresponding 3-D problems with the finite element method and a commercial code. The stresses for the FG structures are found to be in-between those for the homogeneous structures made of the two constituents of the FGM.

1. Introduction

Functionally Graded Materials (FGMs) are a new generation of non-homogeneous composites that have continuous and smooth spatial variations of physical and mechanical properties. In particular, for plates and shell structures studied herein the mechanical properties such as Young's modulus and Poisson's ratio are assumed to vary in the thickness direction according to a predefined relation or the spatial variation of volume fractions of constituents is prescribed. We note that FGMs have been applied and studied in different engineering fields by many researches, e.g. see [1–38]. The practical applications of FGMs have exponentially increased in the last few years, and the mechanics of non-homogeneous solids has received considerable scientific interest as evidenced by numerous publications on the subject. Much of the work on FGMs has been summarized by Shen in his book [1]. Cheng and Batra [2] have correlated deflections of FG polygonal linear elastic plates with those of homogeneous plates of identical geometries and modeled by different plate theories. Yang and Shen [3] have underlined the importance of geometric nonlinearities in bending of shear deformable FG plates. Batra [4] investigated the torsion of axially graded FG cylinders and found the variation of the shear modulus to attain the desired axial variation of the angle of twist per unit length. Vel and Batra [5–7] have provided analytical solutions of the 3D linear elasticity theory for deflections and free vibrations of FG rectangular plates. Deformations of variable thickness FG plates have been studied by Efraim and Eisenberger [8]. Tornabene [9] and Tornabene and Viola [10] introduced the four-parameter power law FG volume fraction which was also used in Refs. [11–13]. Viola et al. [17,21] conducted a parametric investigation of FG cylindrical and conical shells coupled with a stress recovery procedure. Other papers on FG plates and shells include those by Abrate [29,30], Qian et al. [31,32] and Gilhooley et al. [33] who used higher-order shear and normal deformable plate theories of Batra and Vidoli [34] to analyze static and transient deformations of FG rectangular plates.

Most available studies assume that the material properties of FGMs vary either according to an exponential or a power law relation in one or more space directions. In general, the rule of mixtures [9–13] and the Mori–Tanaka scheme [39–42] are often used to evaluate the equivalent mechanical properties of an FGM. It is

* Corresponding author.
E-mail address: francesco.tornabene@unibo.it (F. Tornabene).

[1] http://software.dicam.unibo.it/diqumaspab-project

http://dx.doi.org/10.1016/j.compstruct.2014.08.005

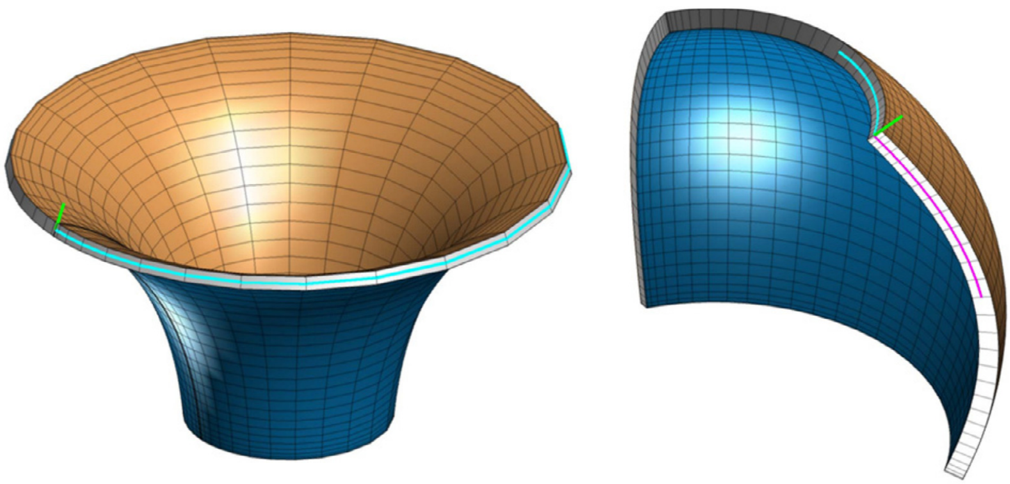

(a) Shell of revolution with free-form meridian (b) Panel of revolution with free-form meridian

Fig. 1. Doubly-curved shells of revolution with C–G–L discretization.

believed that Mori–Tanaka's scheme is more accurate in describing the effective properties of FGMs than the classical rule of mixtures. An advantage of FGMs is that no distinct internal boundaries between different constituents exist because the volume fractions of the two or more materials continuously vary in space. However, if FGMs are produced from particulate composites or by varying the volume fraction of fibers or their orientation in fiber-reinforced composites, then failures from interfacial stress gradients cannot be avoided.

The engineering theories of singly-curved and doubly-curved structures have been refined over the last 70 years [43–117] by Gol'denveizer [45], Novozhilov [46], Kraus [48] and Ventsel and Krauthammer [68]. Leissa [50,51] has extensively studied vibration of plates and shells. Reddy [65,69,70], Qatu [72] and Leissa and Qatu [77] have analyzed deformations of laminated composite shells and plates. The higher-order plate theories are given in the book by Carrera et al. [75], the works by Carrera [82–84], Cho et al. [85], Lo and Christensen [86], and Batra and Vidoli [34]. Most of the recent developments on plate and shell structures can be found in [97–117]. It is recalled that curved shell structures have the major advantage of geometrically coupling the membrane and bending deformations to give strength, stability and toughness

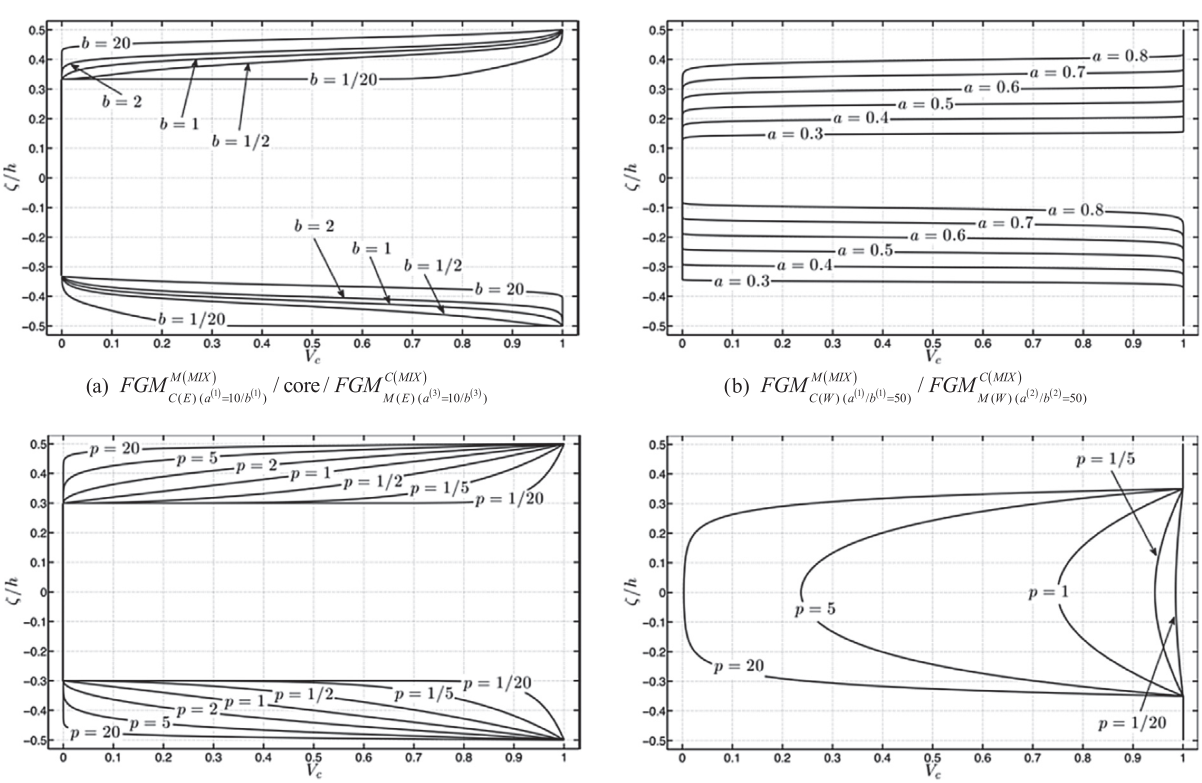

(a) $FGM^{M(MIX)}_{C(E)(a^{(1)}=10/b^{(1)})}$ / core / $FGM^{C(MIX)}_{M(E)(a^{(3)}=10/b^{(3)})}$

(b) $FGM^{M(MIX)}_{C(W)(a^{(1)}/b^{(1)}=50)}$ / $FGM^{C(MIX)}_{M(W)(a^{(2)}/b^{(2)}=50)}$

(c) $FGM^{M(MIX)}_{C(4P)(a^{(1)}=1/b^{(1)}=0/c^{(1)}/p^{(1)})}$ / aluminum/ $FGM^{C(MIX)}_{M(4P)(a^{(3)}=1/b^{(3)}=0/c^{(3)}/p^{(3)})}$

(d) zirconia / $FGM^{M(MIX)}_{C(4P)(a^{(2)}=1/b^{(2)}=1/c^{(2)}=2/p^{(2)})}$ / zirconia

Fig. 2. Through-the-thickness variation of the volume fraction of constituents for different functional forms.

to the structure. The geometrical definitions of singly-curved shells, doubly-curved shells, shells of revolution, and degenerate shells require differential geometry concepts illustrated in the books [79,80]. A general way to define a shell of revolution using Bézier curves is given in [16]. Thus free-form meridians can be geometrically defined for studying unconventional shells of revolution. An engineer can tailor parameters of the Bézier curve to design different structures.

One way to analyze quasistatic deformations of shells is to use an Equivalent Single Layer (ESL) theory because the shell thickness is much smaller than the other two dimensions. Other approaches such as the 3-D elasticity, Eshelby–Stroh formalism [87–89] and the Layer-Wise (LW) theories can be used but they are computationally more expensive than the ESL theory. The ESL theory employed in this work is based on the expansion of the displacement field in the thickness direction to an arbitrary order of the thickness coordinate, and is known as the Carrera Unified Formulation (CUF). This model is general and allows to define several Higher-order Shear Deformation Theories (HSDTs) using a free parameter, and has been employed to study problems for beams, plates and shells [82–84]. It should be added that Murakami's function, also known as the zigzag effect, has been considered. It is needed for sandwich or soft-core structures due to the zigzag behavior of the in-plane displacements among two stiff sheets and a soft core, usually honeycomb or foam materials.

When studying static, free and forced vibrations of rectangular monolithic plates with a higher order shear and normal deformable theory, Qian et al. [31,32] found that the 5th order theory predicts well nearly all aspects of deformations of thick plates given by the 3-D elasticity theory. The classical approach for solving engineering problems involving composite structures is the Finite Element Method (FEM), e.g. see [69,70]. As it is well-known the FEM is based on a weak or variational formulation of the problem. Whereas the basis functions used in the FEM exploit the element connectivity, the basis functions for meshless methods avoid this. Generally, basis functions so generated do not possess the Kronecker delta property, i.e., they do not equal 1 at a node (or a discrete point) and zero at the remaining nodes in the domain.

A particular version of the so-called spectral methods is the Generalized Differential Quadrature (GDQ) method [118–164], which expresses a derivative of a given function as a linear weighted sum of values of the function at discrete points. Thus it can be easily implemented in a computer code. The GDQ is a generalization of the Differential Quadrature Method (DQM) introduced by Bellman et al. in 1971 [119]. Shu [118] applied the GDQ to solve the Navier–Stokes equations, and applications of the DQM to structural mechanics include those of Bert and Malik [120], Striz et al. [121,122] and Chen et al. [123]. Shu [124–129] has also used the GDQ to study vibrations of cylindrical and conical shells. These works have shown that the GDQ method is more stable, accurate and reliable than the DQM for reasons explained in [130–164]. In the last decade the DQM has been further developed to solve different engineering problems, e.g. see the book by Zong and Zhang [130].

The recovery of through-the-thickness variation of stresses from the solution obtained with an ESL theory has been used by Pagano [165] who found the interlaminar stresses by using the Classical Laminated Plate Theory (CLPT) and then integrated with respect to the thickness coordinate the 3-D equilibrium equations. Noor et al. [166] and Malik and Noor [167] developed predictor–corrector procedures to iteratively find to the desired degree of accuracy strains, stresses and displacements throughout a laminate from their values on the laminate mid-surface. Chaudhuri and Seide [168] used shape functions in the thickness direction of each layer to represent the interlaminar stresses.

Sandwich structures are being increasingly used in engineering applications because of their relatively high specific stiffness. Here

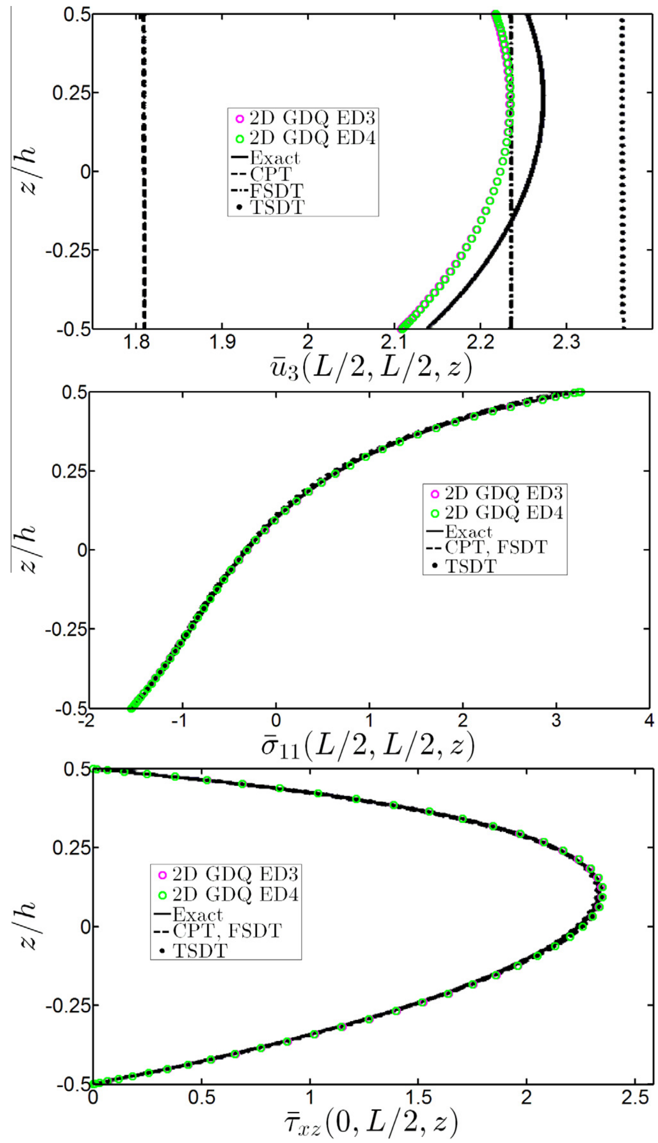

Fig. 3. Comparison of the presently computed through-the-thickness variation of different quantities with those of the semi-analytical solution of [5]; CPT, FSDT and TSDT stand for, respectively, the classical plate theory, first-order shear deformation theory, and the third-order shear deformation theory. Results for these plate theories are taken from [5].

we use the GDQ method and an ESL theory to investigate static deformations of doubly-curved and free-form sandwich shells with either the face sheets or the core made of FGMs with the focus on recovering accurate values of strains and stresses through the thickness of the structure. These values are needed for analyzing the load carrying capacity of a structure and quantifying progressive damage induced in them. The accuracy of the recovered stresses and strains is established by comparing them for a FGM plate with those from an analytical solution of the problem available in the literature [5], and for a sandwich structure with those obtained by numerically analyzing 3-D deformations of the sandwich structure by the finite element method. The materials of the soft-core and the face sheets are assumed to be isotropic and linear elastic. It is found that the ratio of the stiffness of the face sheet to that of the core for which the ESL theory gives reasonably accurate results is higher for a flat sandwich structure than that for a curved sandwich shell.

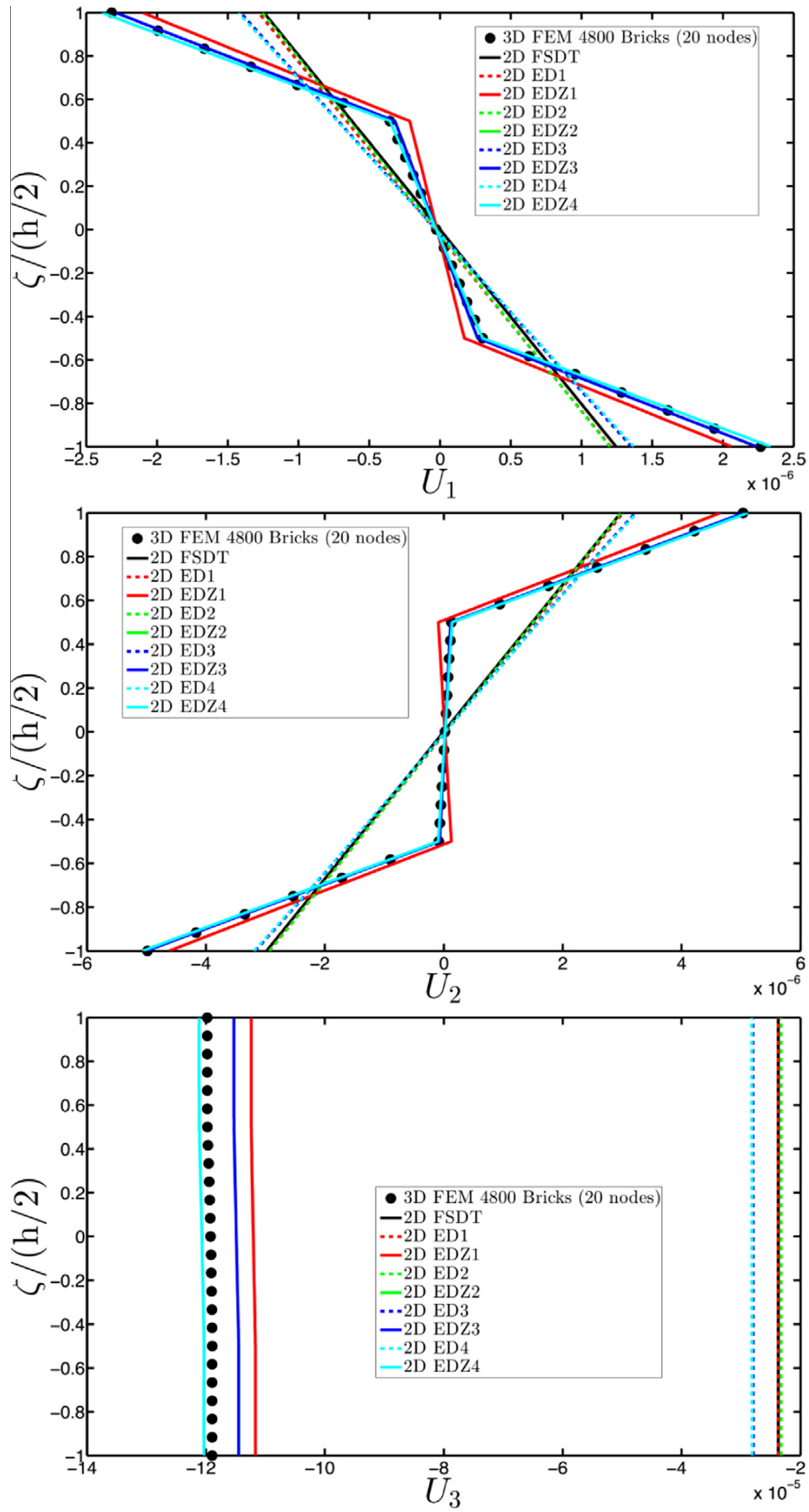

Fig. 4. For a CCFF Zirconia/Core/Zirconia sandwich rectangular plate, through-the-thickness variation of displacements [m] on the transverse normal passing through the point $D = (0.25(\alpha_1^1 - \alpha_1^0), 0.75(\alpha_2^1 - \alpha_2^0))$. The plate has a uniformly distributed load $q_n^{(+)} = -10000$ Pa at the top surface, $h_1 = h_3 = 0.075$ m, $h_2 = 0.15$ m and $E = 0.7$ GPa, $\nu = 0.3$ for the core material.

2. Expressions for volume fractions and homogenization techniques

We analyze static deformations with an ESL HSDT and use equilibrium equations of 3-D elasticity theory to recover through-the-thickness stresses and strains of ceramic–metallic FG shells. The constituent materials and the resulting homogenized material are assumed to be linear elastic and isotropic. Young's modulus $E^{(k)}(\zeta)$ and Poisson's ratio $\nu^{(k)}(\zeta)$ of the kth lamina are assumed to vary continuously and smoothly in the thickness direction ζ. They are functions of the volume fractions and the mechanical properties of the constituent materials. Two different approaches are used to

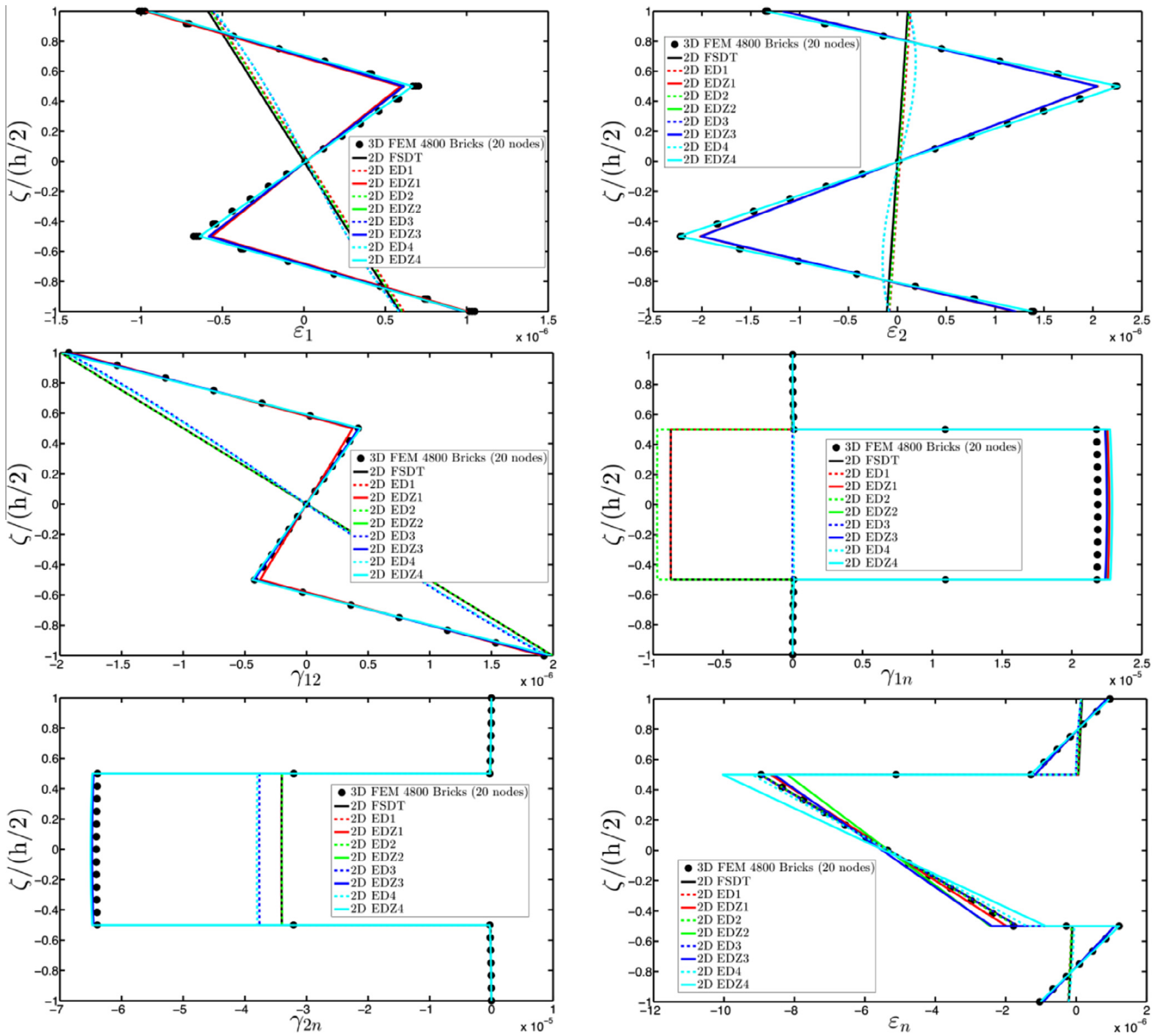

Fig. 5. For a CCFF Zirconia/Core/Zirconia sandwich rectangular plate, through-the-thickness variation of strains on the transverse normal passing through the point $D = (0.25(\alpha_1^1 - \alpha_1^0), 0.75(\alpha_2^1 - \alpha_2^0))$. The plate has a uniformly distributed load $q_n^{(+)} = -10,000$ Pa at the top surface, $h_1 = h_3 = 0.075$ m, $h_2 = 0.15$ m and $E = 0.7$GPa,$\nu = 0.3$ for the core material.

evaluate these mechanical properties: the theory of mixtures [9–13] and the Mori–Tanaka scheme [39–42]. The former is a linear combination of the mechanical properties of the ceramic and the metal constituents weighted by their volume fractions. In the Mori–Tanaka scheme, the bulk modulus, the shear modulus, Young's modulus and Poisson's ratio of the kth lamina are given by

$$K^{(k)}(\zeta) = \left(K_C^{(k)} - K_M^{(k)}\right)\frac{V_C^{(k)}(\zeta)}{1+\left(1-V_C^{(k)}(\zeta)\right)\frac{K_C^{(k)}-K_M^{(k)}}{K_M^{(k)}+\frac{4}{3}G_M^{(k)}}} + K_M^{(k)}$$

$$G^{(k)}(\zeta) = \left(G_C^{(k)} - G_M^{(k)}\right)\frac{V_C^{(k)}(\zeta)}{1+\left(1-V_C^{(k)}(\zeta)\right)\frac{G_C^{(k)}-G_M^{(k)}}{G_M^{(k)}+f_M^{(k)}}} + G_M^{(k)},$$

$$f_M^{(k)} = G_M^{(k)}\frac{9K_M^{(k)}+8G_M^{(k)}}{6K_M^{(k)}+2G_M^{(k)}}$$

$$E^{(k)}(\zeta) = \frac{9K^{(k)}G^{(k)}}{3K^{(k)}+G^{(k)}}, \quad \nu^{(k)}(\zeta) = \frac{3K^{(k)}-2G^{(k)}}{2\left(3K^{(k)}+G^{(k)}\right)} \tag{1}$$

Here subscripts C and M on a quantity imply its values for the ceramic and the metal, respectively. Before proceeding further we give the FGM nomenclature employed in the paper. Effective properties derived by using the Theory of Mixtures and the Mori–Tanaka schemes are denoted, respectively, by superscripts (MIX) and (MT). The four different volume fraction functions considered are the 4 parameters power law ($4P$) [9–13], the Weibull (W), the Exponential (E) and the 3 parameters power law ($3P$) used by Vel and Batra [5]. The acronym used to identify these is: $FGM^{t(\mathrm{th})}_{b(\mathrm{fun})(a^{(k)}/b^{(k)}/\ldots)}$, where t and b represent the material at the top and the bottom of the current lamina (e.g., if the top is made of ceramic and the bottom of metal $t = C$ and $b = M$), (th) = (MIX) or (MT) represents the scheme used to deduce values of the effective material properties, (fun) = ($4P$), (W), (E) or ($3P$) describes the function for through-the-thickness variation of the volume fraction of constituents, and $a^{(k)}/b^{(k)}/\ldots$ are parameters in the expressions for the volume fractions of constituents. For the four parameters $a^{(k)}$, $b^{(k)}$, $c^{(k)}$ and $p^{(k)}$, power law distributions, the volume fraction of the ceramic is given by

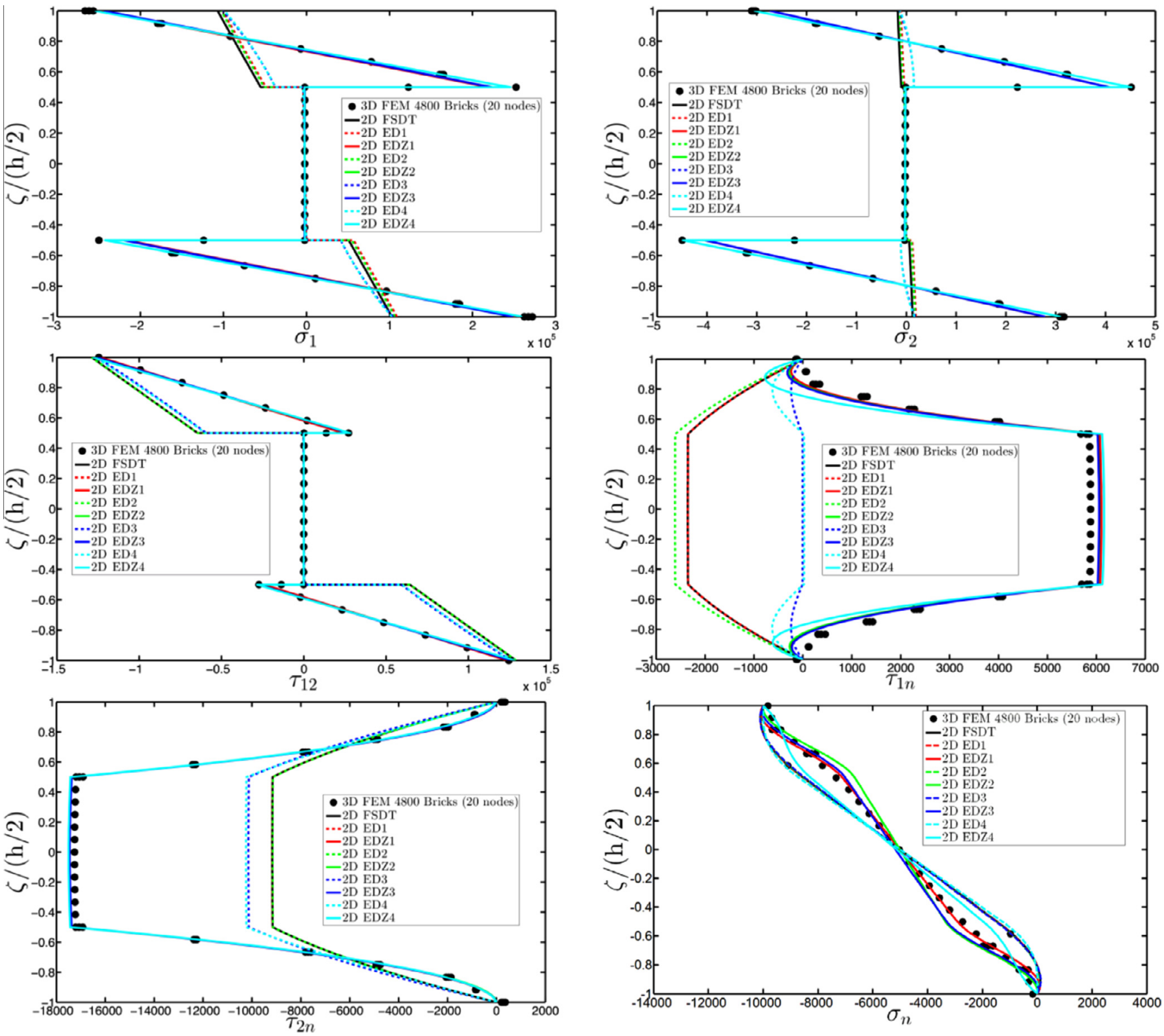

Fig. 6. For a CCFF Zirconia/Core/Zirconia sandwich rectangular plate, through-the-thickness variation of stresses [Pa] on the transverse normal passing through the point $D = \left(0.25\left(\alpha_1^1 - \alpha_1^0\right), 0.75\left(\alpha_2^1 - \alpha_2^0\right)\right)$. The plate has a uniformly distributed load $q_n^{(+)} = -10{,}000$ Pa at the top surface, $h_1 = h_3 = 0.075$ m, $h_2 = 0.15$ m and $E = 0.7$GPa, $\nu = 0.3$ for the core material.

$$V_C^{(k)}(\zeta) = \left(1 - a^{(k)}\left(\frac{\zeta_{k+1} - \zeta}{h_k}\right) + b^{(k)}\left(\frac{\zeta_{k+1} - \zeta}{h_k}\right)^{c^{(k)}}\right)^{p^{(k)}} \quad \text{for } E_t^{(k)} > E_b^{(k)}$$

$$V_C^{(k)}(\zeta) = \left(1 - a^{(k)}\left(\frac{\zeta - \zeta_k}{h_k}\right) + b^{(k)}\left(\frac{\zeta - \zeta_k}{h_k}\right)^{c^{(k)}}\right)^{p^{(k)}} \quad \text{for } E_b^{(k)} > E_t^{(k)} \tag{2}$$

The Weibull distribution (W) is defined by

$$V_C^{(k)}(\zeta) = 1 - \exp\left(-\frac{1}{a^{(k)}}\left(\frac{\zeta - \zeta_k}{h_k}\right)^{b^{(k)}}\right) \quad \text{for } E_t^{(k)} > E_b^{(k)}$$

$$V_C^{(k)}(\zeta) = \exp\left(-\frac{1}{a^{(k)}}\left(\frac{\zeta - \zeta_k}{h_k}\right)^{b^{(k)}}\right) \quad \text{for } E_b^{(k)} > E_t^{(k)} \tag{3}$$

where $a^{(k)}$ and $b^{(k)}$ are parameters. Another two-parameter distribution is the exponential (E) given by

$$V_C^{(k)}(\zeta) = \left(\frac{\exp\left(a^{(k)}\left(\frac{\zeta - \zeta_k}{h_k}\right)\right) - 1}{\left(\exp\left(\frac{a^{(k)}}{2}\right) - 1\right)\left(\exp\left(a^{(k)}\left(\frac{\zeta - \zeta_k}{h_k} - \frac{1}{2}\right)\right) + 1\right)}\right)^{b^{(k)}} \quad \text{for } E_t^{(k)} > E_b^{(k)}$$

$$V_C^{(k)}(\zeta) = 1 - \left(\frac{\exp\left(a^{(k)}\left(\frac{\zeta - \zeta_k}{h_k}\right)\right) - 1}{\left(\exp\left(\frac{a^{(k)}}{2}\right) - 1\right)\left(\exp\left(a^{(k)}\left(\frac{\zeta - \zeta_k}{h_k} - \frac{1}{2}\right)\right) + 1\right)}\right)^{b^{(k)}} \quad \text{for } E_b^{(k)} > E_t^{(k)} \tag{4}$$

The results of the present technique have been compared with the analytical solution of Vel and Batra [5] who used the following expressions for the volume fraction of the ceramic phase

$$V_C^{(k)}(\zeta) = V_C^{-(k)} + \left(V_C^{+(k)} - V_C^{-(k)}\right)\left(\frac{\zeta - \zeta_k}{h_k}\right)^{p^{(k)}} \quad \text{for } E_t^{(k)} > E_b^{(k)}$$

$$V_C^{(k)}(\zeta) = V_C^{-(k)} + \left(V_C^{+(k)} - V_C^{-(k)}\right)\left(\frac{\zeta_{k+1} - \zeta}{h_k}\right)^{p^{(k)}} \quad \text{for } E_b^{(k)} > E_t^{(k)} \tag{5}$$

Table 1
Values of non-dimensional parameterϕ for the (a) FG sandwich plate for which results are reported in Figs. 7–9, using the mean value of the elastic modulus of the sheets and the soft core, considering h_1 = h_3 = 0.05 m and h_2 = 0.2 m, (b) FG fictitious sandwich spherical panel with results reported in Figs. 10–12 using the elastic moduli of the zirconia and the aluminium, considering variable thickness of the sheets and the core, (c) FG sandwich free-form shell for which results are given in Figs. 13–15 using the mean value of the elastic moduli of the face sheets and the stiff core, considering h_1 = h_3 = 0.02 m and h_2 = 0.06 m, (d) FG sandwich free-form panel for which results are displayed in Figs. 16–18 using the mean value of the elastic modulus of the core and the stiff face sheets, considering h_1 = h_3 = 0.01 m and h_2 = 0.08 m.

				Case (a)			
$a^{(1)} = a^{(3)} = 10$	$b^{(1)} = b^{(3)} = b$						
	1/20	1/2	1	2	20		
$\phi^{(-)}$	13.1	50.0	60.1	67.7	87.1		
$\bar{E}^{(-)}$ (GPa)	18.37	70.00	84.18	94.75	122.00		
E_c (GPa)	0.35	0.35	0.35	0.35	0.35		
$\bar{E}^{(+)}$ (GPa)	149.987	122.00	84.18	73.60	46.36		
$\phi^{(+)}$	107.1	87.1	60.1	52.6	33.1		
				Case (b)			
	$b^{(1)} = b^{(2)} = 50$						
$a^{(1)}$	0.3	0.4	0.5	0.6	0.7	0.8	
$a^{(2)}$	0.8	0.7	0.6	0.5	0.4	0.3	
h_s (m)	0.015	0.02	0.025	0.03	0.035	0.04	
h_c (m)	0.035	0.03	0.025	0.02	0.015	0.01	
$\tilde{\phi}$	20.57	32	48	72	112	192	
				Case (c)			
$a^{(1)} = a^{(3)} = 1$, $b^{(1)} = b^{(3)} = 0$, $c^{(1)} = c^{(3)}$	$p^{(1)} = p^{(3)} = p$						
	1/20	1/5	1/2	1	2	5	20
$\bar{E}^{(-)} = \bar{E}^{(+)}$ (GPa)	160.38	147.48	132.12	119	106.99	94.61	83.01
E_c (GPa)	70	70	70	70	70	70	70
ϕ	0.764	0.702	0.629	0.567	0.509	0.451	0.395
				Case (d)			
$a^{(2)} = 1$, $b^{(2)} = 1$, $c^{(2)} = 2$	$p^{(2)} = p$						
	1/20	1/5	1	5	20		
$E^{(-)} = E^{(+)}$ (GPa)	168	168	168	168	168		
$\bar{E}_c$ (GPa)	166.89	163.62	147.84	97.95	49.19		
ϕ	0.13	0.13	0.14	0.21	0.43		

Eq. (3) describes a power-law distribution using 3 parameters $(3P): V_C^{-(k)}, V_C^{+(k)}, p^{(k)}$, where $V_C^{-(k)}$ and $V_C^{+(k)}$ are the ceramic volume fractions on the top and the bottom surfaces of the kth lamina.

3. Higher-order Shear Deformation Theory (HSDT)

A HSDT formulated using both the differential geometry concepts and the mechanics of doubly-curved shells and panels presented in [148–150] is used here. It is an ESL theory in which variables are functions of coordinates of points on the mid-surface of the shell. A shell geometry is limited by $(\alpha_1^0 \leqslant \alpha_1 \leqslant \alpha_1^1)$ along the α_1 – and $(\alpha_2^0 \leqslant \alpha_2 \leqslant \alpha_2^1)$ along the α_2 – coordinate axes that are mutually orthogonal and lie on the mid-surface of the shell, and $(-h/2 \leqslant \zeta \leqslant h/2)$ along the ζ – axis or the shell thickness. The position vector $\mathbf{R}$ of a point in the shell can be expressed as

$$\mathbf{R}(\alpha_1,\alpha_2,\zeta) = \mathbf{r}(\alpha_1,\alpha_2) + \frac{h(\alpha_1,\alpha_2)}{2} z\mathbf{n}(\alpha_1,\alpha_2) \quad \text{for } z = 2\zeta/h(\alpha_1,\alpha_2),\ z \in [-1,1] \tag{6}$$

where $\mathbf{r}(\alpha_1,\alpha_2)$ is the position vector of a point on the mid-surface of the shell and $\mathbf{n}(\alpha_1, \alpha_2)$ is the outward unit normal to the mid-surface. The shell thickness $h(\alpha_1,\alpha_2)$ need not be uniform, and

$$h = \sum_{k=1}^{l} h_k, \quad h_k = \zeta_{k+1} - \zeta_k \tag{7}$$

where h_k is the thickness of the kth lamina. For conciseness, we refer the reader to Refs. [79,80] for the ESL shell theory governing equations in terms of the Lamè parameters A_1, A_2 and the principal radii of curvature R_1, R_2. These equations are valid under a well-known set of assumptions listed in Refs. [148,150] where the CUF of shell theories is provided. The displacement field in the HSDT model of the CUF can be written as

$$\begin{aligned} U_1(\alpha_1,\alpha_2,\zeta) &= F_0 u_1^{(0)} + F_1 u_1^{(1)} + \cdots + F_N u_1^{(N)} + F_{N+1} u_1^{(N+1)} \\ U_2(\alpha_1,\alpha_2,\zeta) &= F_0 u_2^{(0)} + F_1 u_2^{(1)} + \cdots + F_N u_2^{(N)} + F_{N+1} u_2^{(N+1)} \\ U_3(\alpha_1,\alpha_2,\zeta) &= F_0 u_3^{(0)} + F_1 u_3^{(1)} + \cdots + F_N u_3^{(N)} + F_{N+1} u_3^{(N+1)} \end{aligned} \tag{8}$$

or

$$\mathbf{U} = \sum_{\tau=0}^{N+1} \mathbf{F}_\tau \mathbf{u}^{(\tau)} \tag{9}$$

where $\mathbf{U}(\alpha_1,\alpha_2,\zeta) = [U_1\ U_2\ U_3]^T$ is the vector of the displacement components, $\mathbf{u}^{(\tau)}(\alpha_1,\alpha_2) = \left[u_1^{(\tau)}\ u_2^{(\tau)}\ u_3^{(\tau)}\right]^T$ is the τth order vector of the generalized displacements of points on the mid-surface ($\zeta = 0$) of the shell, $\mathbf{F}_\tau$ is the 3×3 matrix

$$\mathbf{F}_\tau = \begin{bmatrix} F_\tau & 0 & 0 \\ 0 & F_\tau & 0 \\ 0 & 0 & F_\tau \end{bmatrix} = F_\tau \mathbf{I}_3, \tag{10}$$

$\mathbf{I}_3$ is the 3×3 identity matrix and $F_\tau(\zeta)$ is a function of the thickness coordinate ζ that can have several forms. The most common form of $F_\tau(\zeta)$ is a polynomial of order $N+1$ such as

$$F_\tau = \begin{cases} \zeta^\tau & \text{for } \tau = 0,1,\ldots,N \\ (-1)^k \left(\frac{2}{\zeta_{k+1}-\zeta_k}\zeta - \frac{\zeta_{k+1}+\zeta_k}{\zeta_{k+1}-\zeta_k}\right) & \text{for } \tau = N+1 \end{cases} \quad \text{for } k = 1,\ldots,l \tag{11}$$

Many other expressions for the thickness function, $F_\tau(\zeta)$, are summarized in Refs. [148–150]. For the displacement field (9), the generalized strain vector, $\boldsymbol{\varepsilon}^{(\tau)}$, is given by

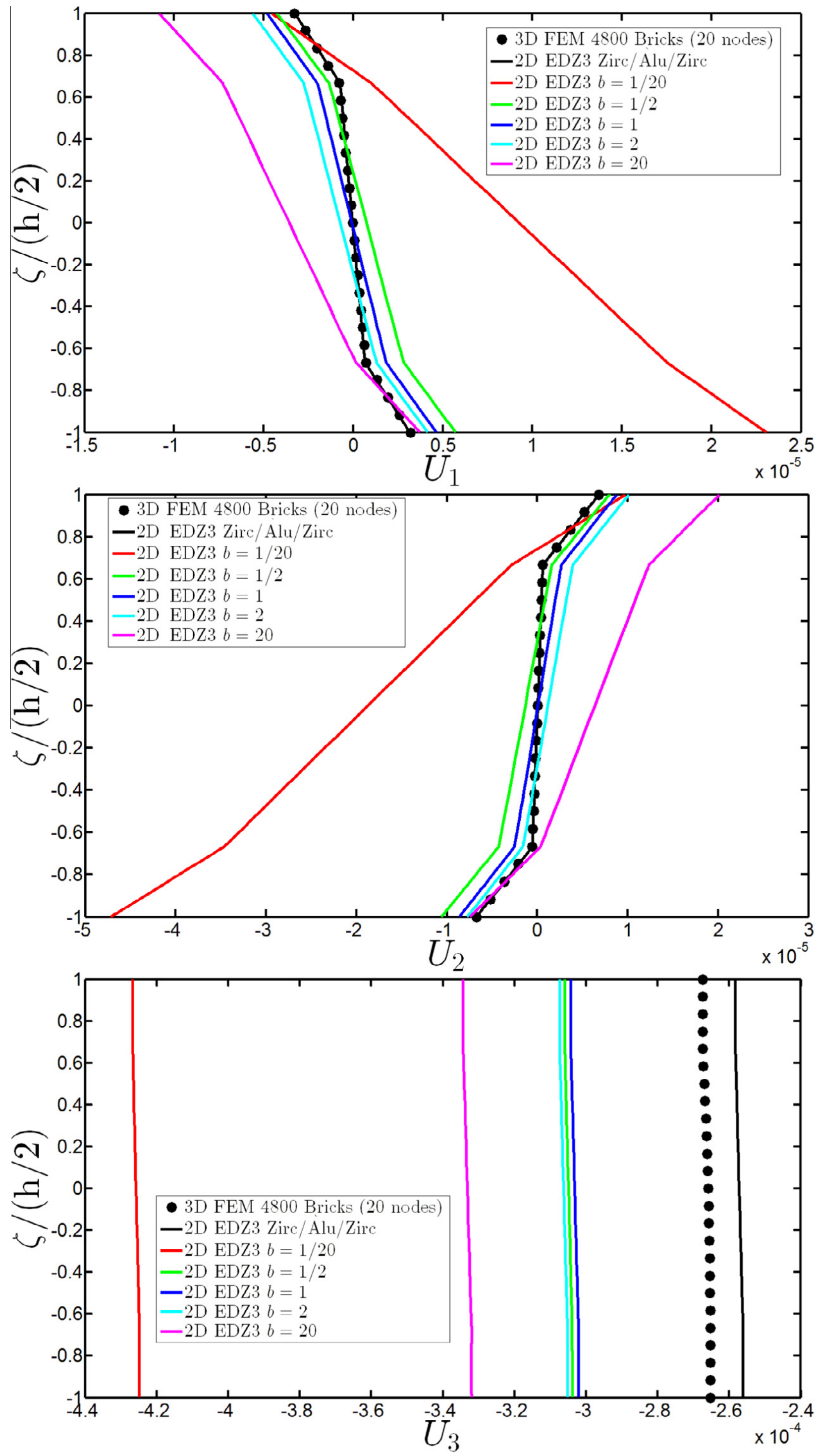

Fig. 7. For a CCFF $FGM^{M(MIX)}_{C(E)(a^{(1)}=10/b^{(1)})}$/Core/$FGM^{C(MIX)}_{M(E)(a^{(3)}=10/b^{(3)})}$ sandwich rectangular plate, through-the-thickness variation of displacement components [m] on the transverse normal passing through the point $D = (0.25(\alpha_1^1 - \alpha_1^0), 0.75(\alpha_2^1 - \alpha_2^0))$. The plate has a uniformly distributed load $q_n^{(+)} = -10,000$ Pa at the top surface, $h_1 = h_3 = 0.05$ m, $h_2 = 0.2$ m, and $E = 0.35$ GPa, $\nu = 0.3$ for the core material.

$$\boldsymbol{\varepsilon}^{(\tau)} = \mathbf{D}_\Omega \mathbf{u}^{(\tau)} \quad \text{for } \tau = 0, 1, 2, \ldots, N, N+1 \tag{12}$$

where $\mathbf{D}_\Omega$ is the differential operator [148,150] involving radii of curvature R_1 and R_2 and derivatives with respect to spatial coordinates α_1 and α_2. It is noted that only $\boldsymbol{\varepsilon}^{(0)}$ and $\boldsymbol{\varepsilon}^{(1)}$ have physical meaning, $\boldsymbol{\varepsilon}^{(\tau)}$ for $\tau = 2, \ldots, N$ represents the generalized parts of the deformation, and $\boldsymbol{\varepsilon}^{(N+1)}$ represents the generalized part of the deformation associated with the zigzag effect. Different generalized strain vectors $\boldsymbol{\varepsilon}^{(\tau)}$ for $\tau = 0, 1, 2, \ldots, N, N+1$, are given by Eq. (12), and the index τ refers to the order of the strain, e.g., $\tau = 1$ represents the first-order deformation. For the linear elastic and isotropic shell material, constitutive equations in terms of stress resultants can be written as

$$\mathbf{S}^{(\tau)} = \sum_{s=0}^{N+1} \mathbf{A}^{(\tau s)} \boldsymbol{\varepsilon}^{(s)} \quad \text{for } \tau = 0, 1, 2, \ldots, N, N+1 \tag{13}$$

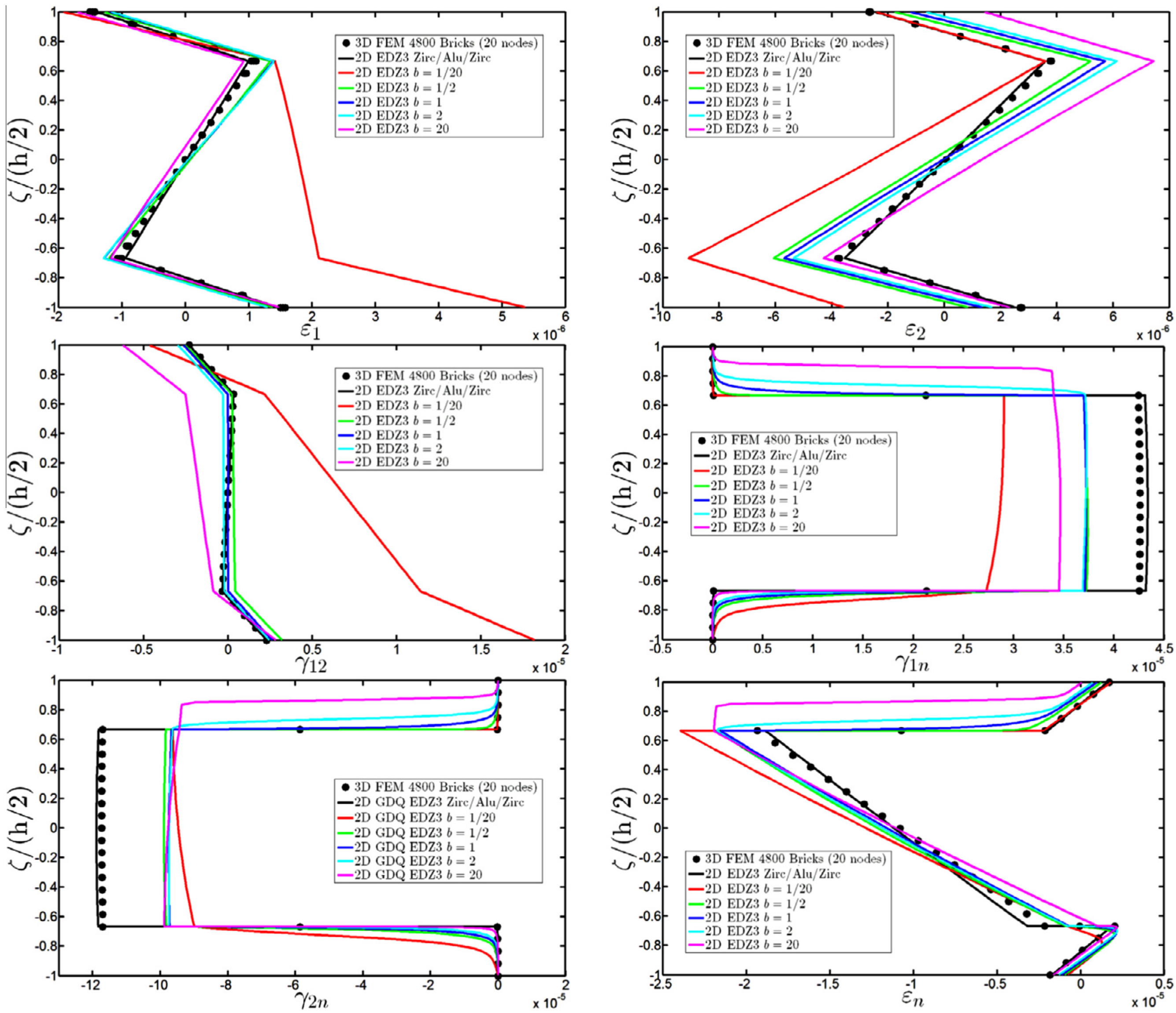

Fig. 8. For a CCFF $FGM^{M(MIX)}_{C(E)(a^{(1)}=10/b^{(1)})}/Core/FGM^{C(MIX)}_{M(E)(a^{(3)}=10/b^{(3)})}$ sandwich rectangular plate, through-the-thickness variation of strains on the transverse normal passing through the point $D = (0.25(\alpha_1^1-\alpha_1^0), 0.75(\alpha_2^1-\alpha_2^0))$. The plate has a uniformly distributed load $q_n^{(+)} = -10,000$ Pa at the top surface, $h_1 = h_3 = 0.05$ m, $h_2 = 0.2$ m, and $E = 0.35$ GPa, $\nu = 0.3$ for the core material.

where $\mathbf{S}^{(\tau)}(\alpha_1,\alpha_2) = \left[N_1^{(\tau)}\ N_2^{(\tau)}\ N_{12}^{(\tau)}\ N_{21}^{(\tau)}\ T_1^{(\tau)}\ T_2^{(\tau)}\ P_1^{(\tau)}\ P_2^{(\tau)}\ S_3^{(\tau)}\right]^T$ is the τth order vector of the stress resultants and $\mathbf{A}^{(\tau s)}$ is the matrix of the elastic constants [148,150] defined as

$$
\begin{aligned}
A_{nm(pq)}^{(\tau s)} &= \sum_{k=1}^{l}\int_{\zeta_k}^{\zeta_{k+1}} \overline{C}_{nm}^{(k)} F_s F_\tau \frac{H_1 H_2}{H_1^p H_2^q}\, d\zeta \\
A_{nm(pq)}^{(\tilde{\tau} s)} &= \sum_{k=1}^{l}\int_{\zeta_k}^{\zeta_{k+1}} \overline{C}_{nm}^{(k)} F_s \frac{\partial F_\tau}{\partial\zeta} \frac{H_1 H_2}{H_1^p H_2^q}\, d\zeta \quad \text{for } \tau, s = 0,1,2,\ldots,N,N+1 \\
&\qquad\qquad\qquad\qquad\qquad\qquad\qquad\quad \text{for } n,m = 1,2,3,4,5,6 \\
A_{nm(pq)}^{(\tau \tilde{s})} &= \sum_{k=1}^{l}\int_{\zeta_k}^{\zeta_{k+1}} \overline{C}_{nm}^{(k)} \frac{\partial F_s}{\partial\zeta} F_\tau \frac{H_1 H_2}{H_1^p H_2^q}\, d\zeta \quad \text{for } p,q = 0,1,2 \\
A_{nm(pq)}^{(\tilde{\tau} \tilde{s})} &= \sum_{k=1}^{l}\int_{\zeta_k}^{\zeta_{k+1}} \overline{C}_{nm}^{(k)} \frac{\partial F_s}{\partial\zeta} \frac{\partial F_\tau}{\partial\zeta} \frac{H_1 H_2}{H_1^p H_2^q}\, d\zeta
\end{aligned}
\tag{14}
$$

Here, superscripts τ, s indicate the corresponding thickness functions F_τ, F_s, respectively. The superscripts $\tilde{\tau}, \tilde{s}$ imply that the corresponding thickness functions F_τ, F_s are replaced by $\frac{\partial F_\tau}{\partial\zeta}, \frac{\partial F_s}{\partial\zeta}$, respectively, p, q are exponents of the quantities $H_1 = 1 + \frac{\zeta}{R_1}$, $H_2 = 1 + \frac{\zeta}{R_2}$, and n, m are indices of the material constants $\overline{C}_{nm}^{(k)}$ defined for the kth lamina. Expressions for material constants $\overline{C}_{nm}^{(k)}$ can be found in structural mechanics books [65,69,70].

Using the principle of minimum potential energy [79,80], equations of static equilibrium can be written as

$$
\mathbf{D}_\Omega^* \mathbf{S}^{(\tau)} + \mathbf{q}^{(\tau)} = \mathbf{0} \quad \text{for } \tau = 0,1,2,\ldots,N,N+1 \tag{15}
$$

where $\mathbf{D}_\Omega^*$ is the differential operator [148,150], $\mathbf{q}^{(\tau)} = \left[q_1^{(\tau)}\quad q_2^{(\tau)}\quad q_n^{(\tau)}\right]^T$ is the static load equivalent to forces applied on the shell top and bottom surfaces, and

$$
\begin{aligned}
q_1^{(\tau)} &= q_1^{(-)} F_\tau^{(-)} H_1^{(-)} H_2^{(-)} + q_1^{(+)} F_\tau^{(+)} H_1^{(+)} H_2^{(+)} \\
q_2^{(\tau)} &= q_2^{(-)} F_\tau^{(-)} H_1^{(-)} H_2^{(-)} + q_2^{(+)} F_\tau^{(+)} H_1^{(+)} H_2^{(+)} \quad \text{for } \tau = 0,1,2,\ldots,N,N+1 \\
q_n^{(\tau)} &= q_n^{(-)} F_\tau^{(-)} H_1^{(-)} H_2^{(-)} + q_n^{(+)} F_\tau^{(+)} H_1^{(+)} H_2^{(+)}
\end{aligned}
\tag{16}
$$

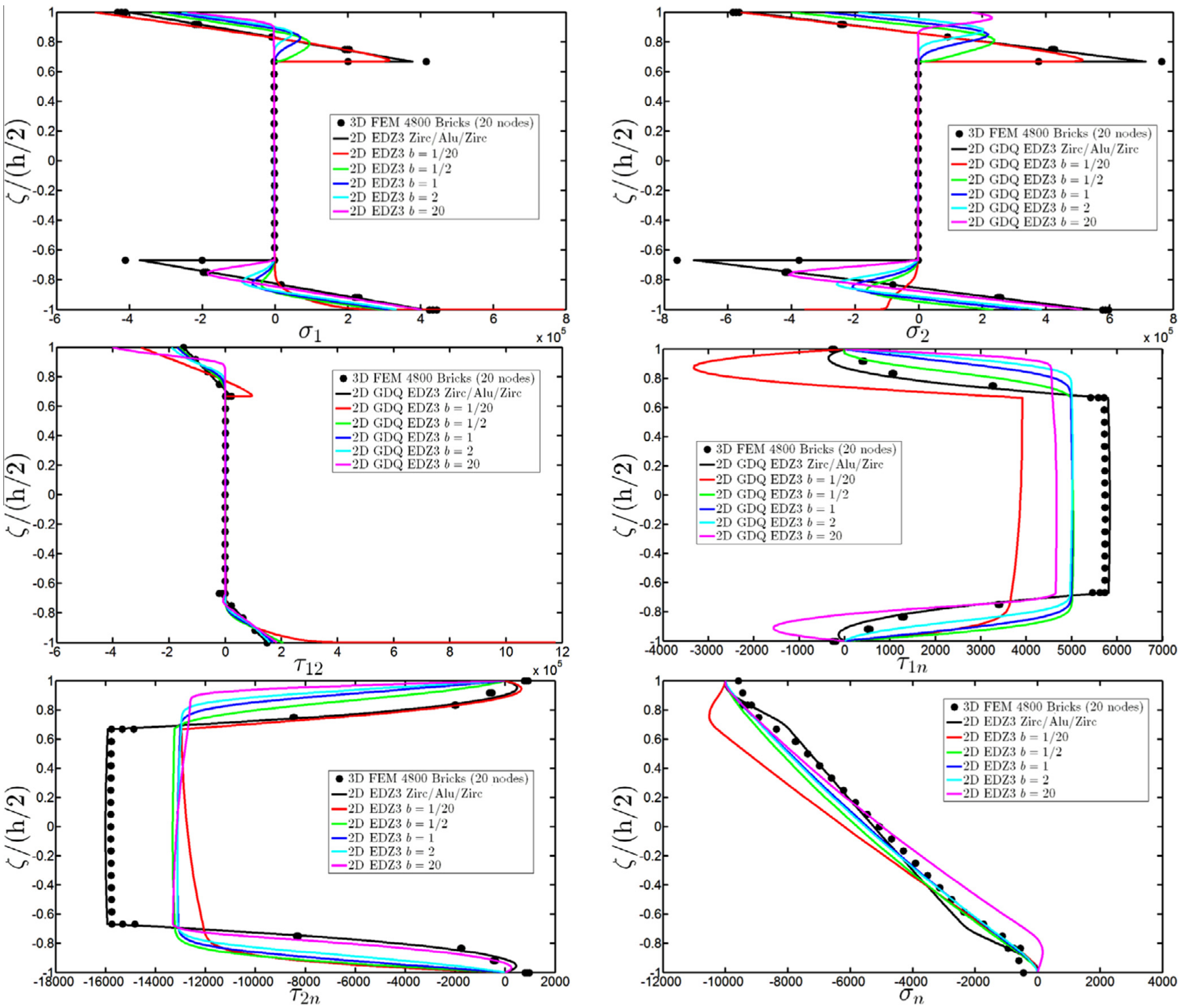

Fig. 9. For a CCFF $FGM^{M(MIX)}_{C(E)(a^{(1)}=10/b^{(1)})}$/Core/$FGM^{C(MIX)}_{M(E)(a^{(3)}=10/b^{(3)})}$ sandwich rectangular plate, through-the-thickness variation of strains on the transverse normal passing through the point $D = (0.25(\alpha_1^1 - \alpha_1^0), 0.75(\alpha_2^1 - \alpha_2^0))$. The plate has a uniformly distributed load $q_n^{(+)} = -10,000$ Pa at the top surface, $h_1 = h_3 = 0.05$ m, $h_2 = 0.2$ m, and $E = 0.35$GPa, $\nu = 0.3$ for the core material.

Here $q_1^{(-)}, q_2^{(-)}, q_n^{(-)}$ and $q_1^{(+)}, q_2^{(+)}, q_n^{(+)}$ are surface tractions applied on the bottom, $\zeta = -h/2$, and the top, $\zeta = +h/2$, surfaces, respectively. Combining Eqs. (12), (13) and (15), the governing equations can be written in terms of generalized displacements as

$$\sum_{s=0}^{N+1} \mathbf{L}^{(\tau s)}\mathbf{u}^{(s)} + \mathbf{q}^{(\tau)} = \mathbf{0} \quad \text{for } \tau = 0,1,2,\ldots,N,N+1 \tag{17}$$

where $\mathbf{L}^{(\tau s)} = \mathbf{D}_\Omega^* \mathbf{A}^{(\tau s)} \mathbf{D}_\Omega$ is the equilibrium operator [148,150]. The total number of equations depends on the order of expansion τ. Boundary conditions for differential equations (17) for clamped (C), simply-supported (S) and free (F) edges are listed below.

Clamped edge (C)

$$u_1^{(\tau)} = u_2^{(\tau)} = u_3^{(\tau)} = 0 \quad \text{for } \tau = 0,1,2,\ldots,N,N+1, \quad \text{at} \quad \alpha_1 = \alpha_1^0 \text{ or } \alpha_1 = \alpha_1^1,\ \alpha_2^0 \leqslant \alpha_2 \leqslant \alpha_2^1 \tag{18}$$

$$u_1^{(\tau)} = u_2^{(\tau)} = u_3^{(\tau)} = 0 \quad \text{for } \tau = 0,1,2,\ldots,N,N+1, \quad \text{at} \quad \alpha_2 = \alpha_2^0 \text{ or } \alpha_2 = \alpha_2^1,\ \alpha_1^0 \leqslant \alpha_1 \leqslant \alpha_1^1 \tag{19}$$

Simply-supported edge (S)

$$N_1^{(\tau)} = 0, u_2^{(\tau)} = u_3^{(\tau)} = 0 \quad \text{for } \tau = 0,1,2,\ldots,N,N+1, \quad \text{at} \quad \alpha_1 = \alpha_1^0 \text{ or } \alpha_1 = \alpha_1^1,\ \alpha_2^0 \leqslant \alpha_2 \leqslant \alpha_2^1 \tag{20}$$

$$N_2^{(\tau)} = 0, u_1^{(\tau)} = u_3^{(\tau)} = 0, \quad \text{for } \tau = 0,1,2,\ldots,N,N+1, \quad \text{at} \quad \alpha_2 = \alpha_2^0 \text{ or } \alpha_2 = \alpha_2^1,\ \alpha_1^0 \leqslant \alpha_1 \leqslant \alpha_1^1 \tag{21}$$

Free edge (F)

$$N_1^{(\tau)} = 0, N_{12}^{(\tau)} = 0, T_1^{(\tau)} = 0 \quad \text{for } \tau = 0,1,2,\ldots,N,N+1, \quad \text{at} \quad \alpha_1 = \alpha_1^0 \text{ or } \alpha_1 = \alpha_1^1,\ \alpha_2^0 \leqslant \alpha_2 \leqslant \alpha_2^1 \tag{22}$$

$$N_{21}^{(\tau)} = 0, N_2^{(\tau)} = 0, T_2^{(\tau)} = 0 \quad \text{for } \tau = 0,1,2,\ldots,N,N+1, \quad \text{at} \quad \alpha_2 = \alpha_2^0 \text{ or } \alpha_2 = \alpha_2^1,\ \alpha_1^0 \leqslant \alpha_1 \leqslant \alpha_1^1 \tag{23}$$

In general, a panel is defined by four edges. However, the given geometric description allows considering shells of revolution, in other words structures which have a closing meridian (shells). For these

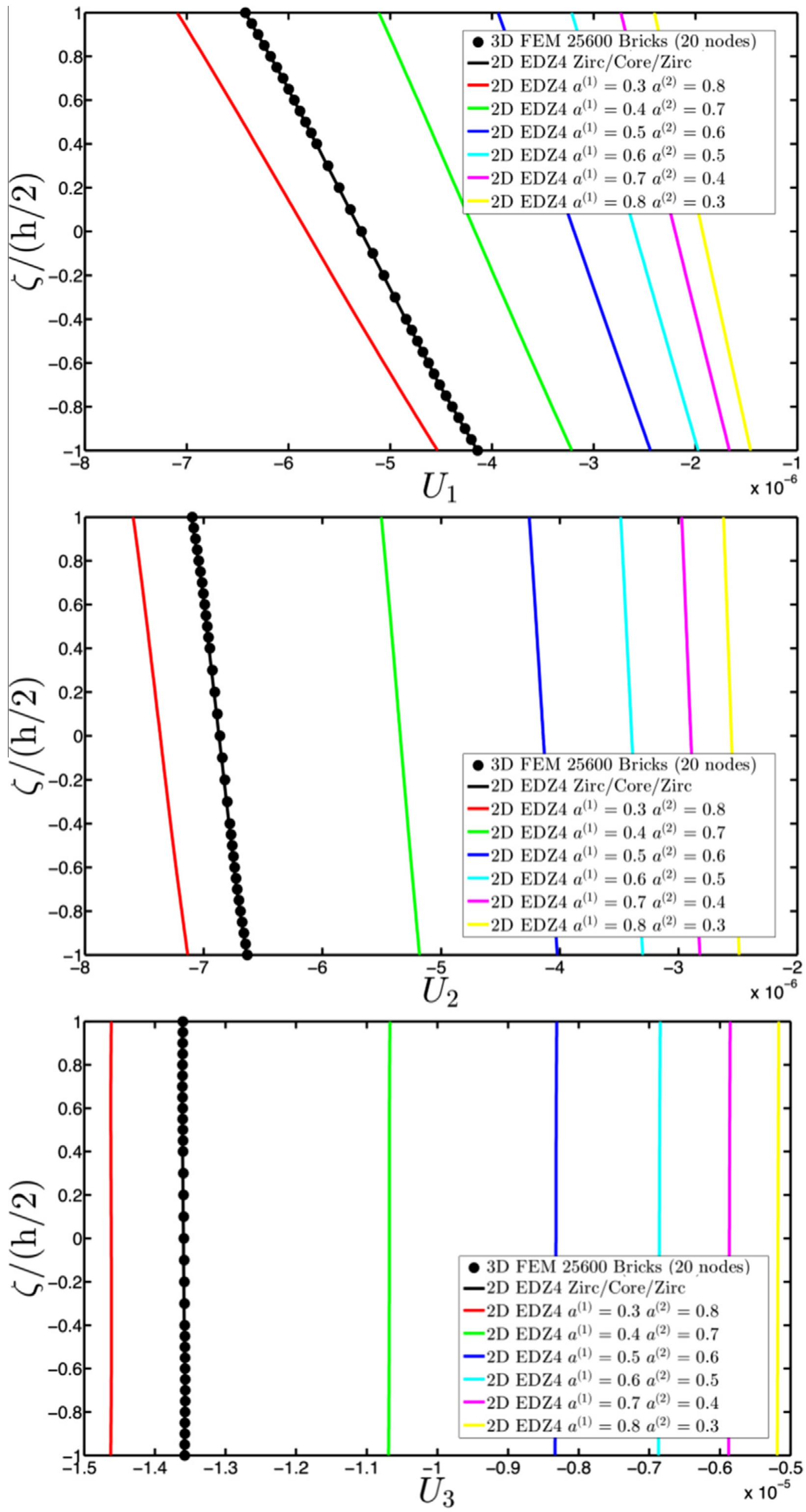

Fig. 10. For a FCFF $FGM^{M(MIX)}_{C(W)(a^{(1)}/b^{(1)}=50)}/FGM^{C(MIX)}_{M(W)(a^{(2)}/b^{(2)}=50)}$ spherical panel, through-the-thickness variation of displacement components [m] on the transverse normal passing through the point $C = (0.25(\alpha_1^1 - \alpha_1^0), 0.25(\alpha_2^1 - \alpha_2^0))$. The panel has a uniformly distributed load $q_n^{(+)} = -10,000$ Pa at the top surface, $h_1 = h_2 = 0.05$ m.

structures the continuity of displacements and surface tractions at $\alpha_2 = 0{,}2\pi$ is enforced

Kinematic (displacement) compatibility conditions along the closing meridian ($\alpha_2 = 0{,}2\pi$)

$$u_1^{(\tau)}(\alpha_1, 0, t) = u_1^{(\tau)}(\alpha_1, 2\pi, t), \quad u_2^{(\tau)}(\alpha_1, 0, t) = u_2^{(\tau)}(\alpha_1, 2\pi, t),$$
$$u_3^{(\tau)}(\alpha_1, 0, t) = u_3^{(\tau)}(\alpha_1, 2\pi, t) \quad \text{for } \tau = 0, 1, 2, \dots, N, N+1,$$
$$\alpha_1^0 \leqslant \alpha_1 \leqslant \alpha_1^1 \tag{24}$$

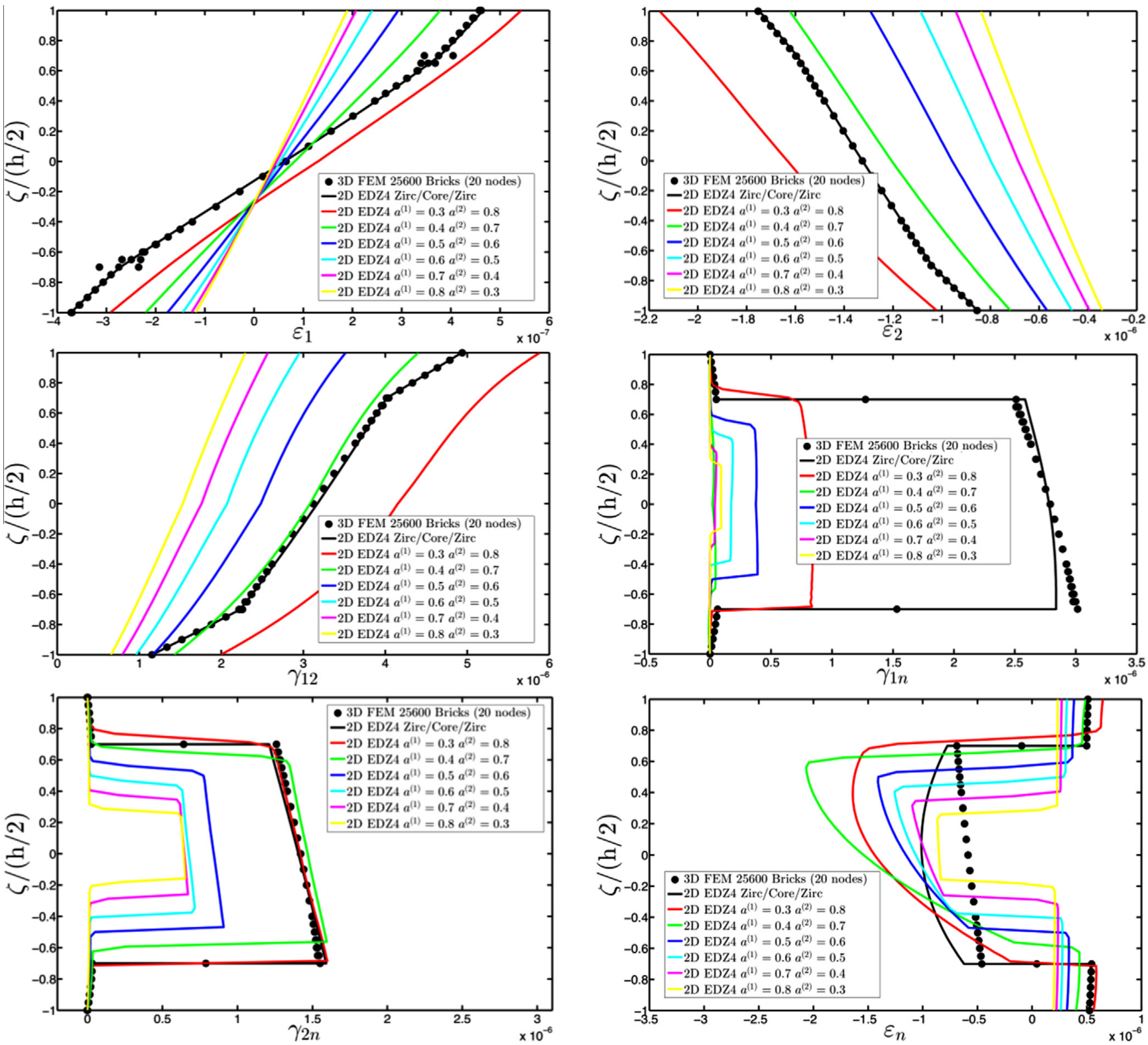

Fig. 11. For a FCFF $FGM^{M(MIX)}_{C(W)(a^{(1)}/b^{(1)}=50)}/FGM^{C(MIX)}_{M(W)(a^{(2)}/b^{(2)}=50)}$ spherical panel, through-the-thickness variation of strains on the transverse normal passing through the point $C=(0.25(\alpha_1^1-\alpha_1^0),0.25(\alpha_2^1-\alpha_2^0))$. The panel has a uniformly distributed load $q_n^{(+)}=-10,000$ Pa at the top surface, $h_1=h_2=0.05$ m.

Physical (surface tractions) compatibility conditions along the closing meridian($\alpha_2=0,2\pi$)

$$N_{21}^{(\tau)}(\alpha_1,0,t)=N_{21}^{(\tau)}(\alpha_1,2\pi,t),\quad N_2^{(\tau)}(\alpha_1,0,t)=N_2^{(\tau)}(\alpha_1,2\pi,t),$$
$$T_2^{(\tau)}(\alpha_1,0,t)=T_2^{(\tau)}(\alpha_1,2\pi,t)\quad \text{for } \tau=0,1,2,\ldots,N,N+1,$$
$$\alpha_1^0\leqslant\alpha_1\leqslant\alpha_1^1 \tag{25}$$

4. Approximate numerical solution

The boundary-value problem (BVP) formulated above is numerically solved by using the GDQ method that transforms a partial or a total derivative of an unknown function into an algebraic form, (e.g., see Eq. (26)), and hence differential equations into algebraic equations that can be numerically solved for the unknown quantities

$$\left.\frac{\partial^n f(x)}{\partial x^n}\right|_{x=x_m}=\sum_{k=1}^{T}\varsigma_{mk}^{(n)}f(x_k), \tag{26}$$

Furthermore, the GDQ method can be used to approximate integrals as reported in several papers [148–150,160]. This approximation, termed Generalized Integral Quadrature (GIQ) rule [118], is employed in the present work for approximating the engineering constants $A_{nm(pq)}^{(\tau s)},A_{nm(pq)}^{(\tilde{\tau} s)},A_{nm(pq)}^{(\tau\tilde{s})},A_{nm(pq)}^{(\tilde{\tau}\tilde{s})}$. We note that the SSPH method proposed by Zhang and Batra [169,170] also expresses derivatives of a function at a point in terms of values of the function at its neighboring points. The SSPH basis functions have been employed to numerically analyze several BVPs [169–171]. For numerically solving the BVP a Chebyshev–Gauss–Lobatto (C–G–L) grid of points is considered both in the interior and at boundaries of the shell/panel. That is, coordinates $(\alpha_{1i},\alpha_{2j})$ of points on the reference surface are given by

$$\begin{aligned}\alpha_{1i}&=\left(1-\cos\left(\frac{i-1}{I_N-1}\pi\right)\right)\frac{(\alpha_1^1-\alpha_1^0)}{2}+\alpha_1^0,\quad i=1,2,\ldots,I_N,\quad \text{for } \alpha_1\in[\alpha_1^0,\alpha_1^1]\\ \alpha_{2j}&=\left(1-\cos\left(\frac{j-1}{I_M-1}\pi\right)\right)\frac{(\alpha_2^1-\alpha_2^0)}{2}+\alpha_2^0,\quad j=1,2,\ldots,I_M,\quad \text{for } \alpha_2\in[\alpha_2^0,\alpha_2^1]\end{aligned} \tag{27}$$

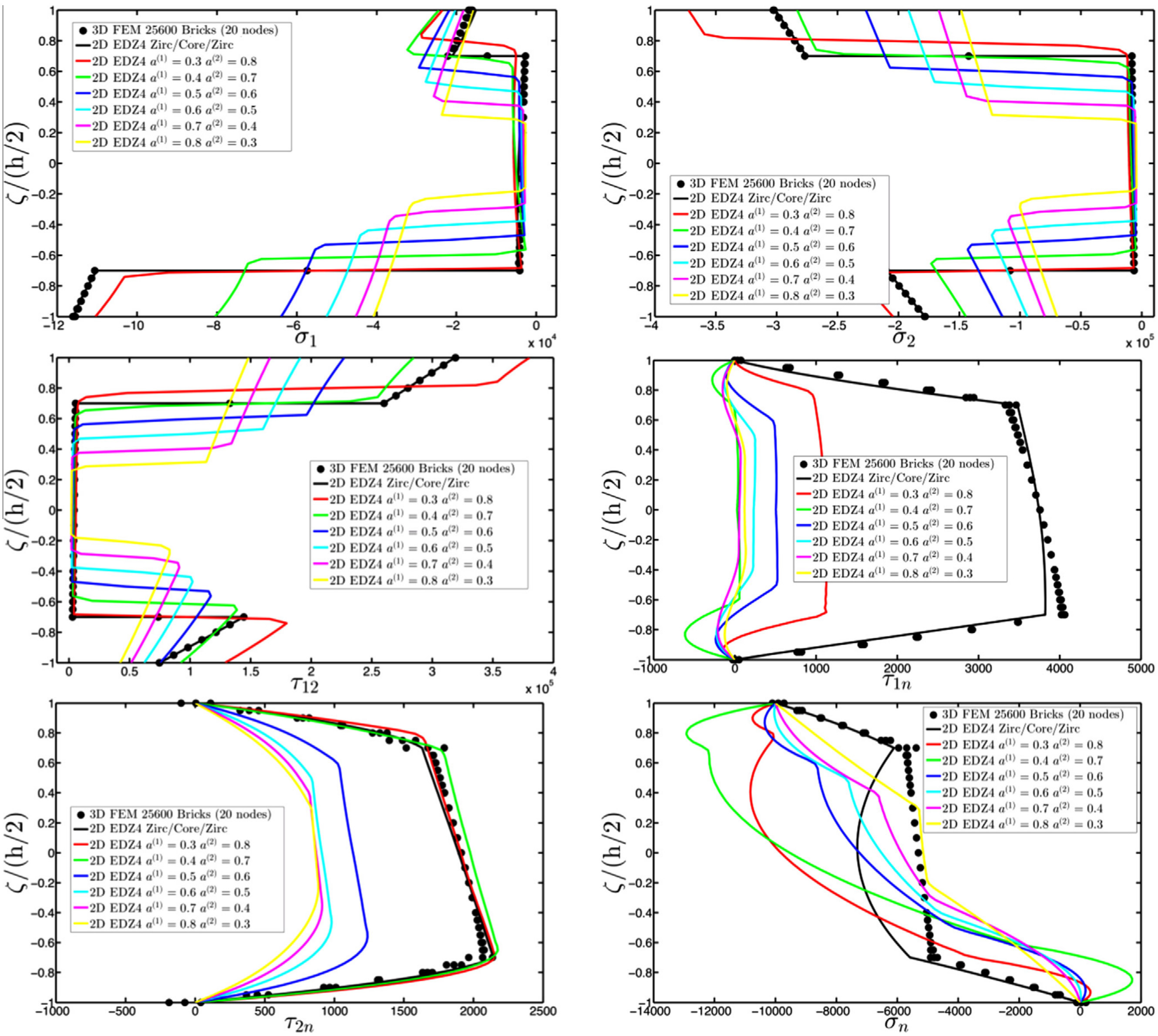

Fig. 12. For a FCFF $FGM^{M(MIX)}_{C(W)(a^{(1)}/b^{(1)}=50)}/FGM^{C(MIX)}_{M(W)(a^{(2)}/b^{(2)}=50)}$ spherical panel, through-the-thickness variation of stresses [Pa] on the transverse normal passing through the point $C = (0.25(\alpha_1^1 - \alpha_1^0), 0.25(\alpha_2^1 - \alpha_2^0))$. The panel has a uniformly distributed load $q_n^{(+)} = -10,000$ Pa at the top surface, $h_1 = h_2 = 0.05$ m.

where I_N, I_M are the total number of sampling points used to discretize the domain in the α_1, α_2 directions, respectively. It is shown in Refs. [127–129,131–140] that the C–G–L points give accurate results. Using Eq. (26), the BVP defined by Eqs. (17)–(25) can be written as the following system of algebraic equations

$$\begin{bmatrix} \mathbf{K}_{bb} & \mathbf{K}_{bd} \\ \mathbf{K}_{db} & \mathbf{K}_{dd} \end{bmatrix} \begin{bmatrix} \boldsymbol{\delta}_b \\ \boldsymbol{\delta}_d \end{bmatrix} - \begin{bmatrix} \mathbf{f}_b \\ \mathbf{f}_d \end{bmatrix} = \begin{bmatrix} \mathbf{0} \\ \mathbf{0} \end{bmatrix} \tag{28}$$

In Eq. (28) subscripts b and d in $\boldsymbol{\delta} = [\boldsymbol{\delta}_b \; \boldsymbol{\delta}_d]^T$ refer to degrees of freedom associated with the boundary $\boldsymbol{\delta}_b$ where surface tractions are prescribed and the domain $\boldsymbol{\delta}_d$, respectively. We note that null displacements prescribed at points on the clamped boundary have been incorporated in Eq. (28). Using the static condensation on the first line of (28) we obtain

$$\boldsymbol{\delta}_b = (\mathbf{K}_{bb})^{-1}[\mathbf{f}_b - \mathbf{K}_{bd}\boldsymbol{\delta}_d] \tag{29}$$

Substituting from Eq. (29) into Eq. (28) we get

$$\left(\mathbf{K}_{dd} - \mathbf{K}_{db}(\mathbf{K}_{bb})^{-1}\mathbf{K}_{bd}\right)\boldsymbol{\delta}_d = \mathbf{f}_d - \mathbf{K}_{db}(\mathbf{K}_{bb})^{-1}\mathbf{f}_b \tag{30}$$

which can be written as

$$\overline{\mathbf{K}}\boldsymbol{\delta}_d = \bar{\mathbf{f}} \tag{31}$$

where $\overline{\mathbf{K}} = \mathbf{K}_{dd} - \mathbf{K}_{db}(\mathbf{K}_{bb})^{-1}\mathbf{K}_{bd}$ and $\bar{\mathbf{f}} = \mathbf{f}_d - \mathbf{K}_{db}(\mathbf{K}_{bb})^{-1}\mathbf{f}_b$. The system of linear equations (31) can be easily solved. The GDQ method is computationally cost effective since no integration on the 2-D domain is needed.

5. Recovery of transverse stresses and strains

As in previous studies [139,140,146–150,157,158,160,161] on posteriori recovery of transverse shear and normal stresses, we use the 3-D linear elasticity equilibrium equations (32) for a general doubly-curved shell to compute these stresses. Even though the 2-D shell problem formulated above considers through-the-thickness stresses, they may not satisfy surface tractions prescribed on the top and the bottom surfaces. Hence, Eq. (32) can be used to evaluate or correct all transverse normal and shear strains and stresses

$$
\begin{aligned}
\frac{\partial \tau_{1n}}{\partial \zeta}+\tau_{1n}\left(\frac{2}{R_1+\zeta}+\frac{1}{R_2+\zeta}\right) &= -\frac{1}{A_1(1+\zeta/R_1)}\frac{\partial \sigma_1}{\partial \alpha_1}+\frac{\sigma_2-\sigma_1}{A_1A_2(1+\zeta/R_2)}\frac{\partial A_2}{\partial \alpha_1} \\
&\quad -\frac{1}{A_2(1+\zeta/R_2)}\frac{\partial \tau_{12}}{\partial \alpha_2}-\frac{2\tau_{12}}{A_1A_2(1+\zeta/R_1)}\frac{\partial A_1}{\partial \alpha_2} \\
\frac{\partial \tau_{2n}}{\partial \zeta}+\tau_{2n}\left(\frac{1}{R_1+\zeta}+\frac{2}{R_2+\zeta}\right) &= -\frac{1}{A_2(1+\zeta/R_2)}\frac{\partial \sigma_2}{\partial \alpha_2}+\frac{\sigma_1-\sigma_2}{A_1A_2(1+\zeta/R_1)}\frac{\partial A_1}{\partial \alpha_2} \\
&\quad -\frac{1}{A_1(1+\zeta/R_1)}\frac{\partial \tau_{12}}{\partial \alpha_1}-\frac{2\tau_{12}}{A_1A_2(1+\zeta/R_2)}\frac{\partial A_2}{\partial \alpha_1} \\
\frac{\partial \sigma_n}{\partial \zeta}+\sigma_n\left(\frac{1}{R_1+\zeta}+\frac{1}{R_2+\zeta}\right) &= -\frac{1}{A_1(1+\zeta/R_1)}\frac{\partial \tau_{1n}}{\partial \alpha_1}-\frac{\tau_{1n}}{A_1A_2(1+\zeta/R_2)}\frac{\partial A_2}{\partial \alpha_1} \\
&\quad -\frac{1}{A_2(1+\zeta/R_2)}\frac{\partial \tau_{2n}}{\partial \alpha_2}-\frac{\tau_{2n}}{A_1A_2(1+\zeta/R_1)}\frac{\partial A_1}{\partial \alpha_2} \\
&\quad +\frac{\sigma_1}{R_1+\zeta}+\frac{\sigma_2}{R_2+\zeta}
\end{aligned} \tag{32}
$$

Note that the in-plane stresses $\sigma_1,\sigma_2,\tau_{12}$ and their derivatives $\frac{\partial \sigma_1}{\partial \alpha_1},\frac{\partial \sigma_2}{\partial \alpha_2},\frac{\partial \tau_{12}}{\partial \alpha_1},\frac{\partial \tau_{12}}{\partial \alpha_2}$ are known at all points of the 3-D solid shell. Eq. (32) are solved for the transverse shear and the transverse normal stresses, $\tau_{1n},\tau_{2n},\sigma_n$, by using the GDQ method along the thickness direction ζ at the C–G–L points given by

$$
\zeta_m=\left(1-\cos\left(\frac{m-1}{I_T-1}\pi\right)\right)\frac{h}{2}-\frac{h}{2},\quad m=1,2,\ldots,I_T, \quad \text{for } \zeta\in\left[-\frac{h}{2},\frac{h}{2}\right] \tag{33}
$$

Eq. $(32)_3$ is solved for σ_n only after the numerical evaluation of the two shear stresses τ_{1n},τ_{2n} and their derivatives $\frac{\partial \tau_{1n}}{\partial \alpha_1},\frac{\partial \tau_{2n}}{\partial \alpha_2}$, e.g. see Refs. [138,160]. When solving Eq. (32) for the transverse shear stresses τ_{1n},τ_{2n}, the traction boundary conditions at the bottom surface are first used and a linear correction is employed afterwards for the satisfaction of the traction boundary conditions at the top surface as exemplified below in Eqs. (34) and (35).

$$
\begin{cases}
\tau_{1n(ij1)}=\bar{q}^{(-)}_{1(ij)}\,\text{(Boundary condition at the bottom surface of the shell)} \\
\displaystyle\sum_{k=1}^{I_T}\varsigma^{\zeta(1)}_{mk}\tau_{1n(ijk)}+\tau_{1n(ijm)}\left(\frac{2}{R_{1(ij)}+\zeta_m}+\frac{1}{R_{2(ij)}+\zeta_m}\right)=-\frac{1}{A_{1(ij)}\left(1+\zeta_m/R_{1(ij)}\right)}\left.\frac{\partial \sigma_1}{\partial \alpha_1}\right|_{(ijm)} \\
\displaystyle+\frac{\sigma_{2(ijm)}-\sigma_{1(ijm)}}{A_{1(ij)}A_{2(ij)}\left(1+\zeta_m/R_{2(ij)}\right)}\left.\frac{\partial A_2}{\partial \alpha_1}\right|_{(ij)}+ \\
\displaystyle-\frac{1}{A_{2(ij)}\left(1+\zeta_m/R_{2(ij)}\right)}\left.\frac{\partial \tau_{12}}{\partial \alpha_2}\right|_{(ijm)}-\frac{2\tau_{12(ijm)}}{A_{1(ij)}A_{2(ij)}\left(1+\zeta_m/R_{1(ij)}\right)}\left.\frac{\partial A_1}{\partial \alpha_2}\right|_{(ij)} \qquad \text{for } m=2,\ldots,I_T
\end{cases}
$$

$$
\begin{cases}
\tau_{2n(ij1)}=\bar{q}^{(-)}_{2(ij)}\,\text{(Boundary condition at the bottom surface of the shell)} \\
\displaystyle\sum_{k=1}^{I_T}\varsigma^{\zeta(1)}_{mk}\tau_{2n(ijk)}+\tau_{2n(ijm)}\left(\frac{1}{R_{1(ij)}+\zeta_m}+\frac{2}{R_{2(ij)}+\zeta_m}\right)=-\frac{1}{A_{2(ij)}\left(1+\zeta_m/R_{2(ij)}\right)}\left.\frac{\partial \sigma_2}{\partial \alpha_2}\right|_{(ijm)} \\
\displaystyle+\frac{\sigma_{1(ijm)}-\sigma_{2(ijm)}}{A_{1(ij)}A_{2(ij)}\left(1+\zeta_m/R_{1(ij)}\right)}\left.\frac{\partial A_1}{\partial \alpha_2}\right|_{(ij)}+ \\
\displaystyle-\frac{1}{A_{1(ij)}\left(1+\zeta_m/R_{1(ij)}\right)}\left.\frac{\partial \tau_{12}}{\partial \alpha_1}\right|_{(ijm)}-\frac{2\tau_{12(ijm)}}{A_{1(ij)}A_{2(ij)}\left(1+\zeta_m/R_{2(ij)}\right)}\left.\frac{\partial A_2}{\partial \alpha_1}\right|_{(ij)} \qquad \text{for } m=2,\ldots,I_T
\end{cases}
$$

The boundary conditions at the top surface of the shell, $\tau_{1n(ijT)}=\bar{q}^{(+)}_{1(ij)}$ and $\tau_{2n(ijT)}=\bar{q}^{(+)}_{2(ij)}$, are satisfied as follows

$$
\begin{aligned}
\bar{\tau}_{1n(ijm)} &= \tau_{1n(ijm)}+\frac{\bar{q}^{(+)}_{1(ij)}-\tau_{1n(ijT)}}{h}\left(\zeta_m+\frac{h}{2}\right) \\
\bar{\tau}_{2n(ijm)} &= \tau_{2n(ijm)}+\frac{\bar{q}^{(+)}_{2(ij)}-\tau_{2n(ijT)}}{h}\left(\zeta_m+\frac{h}{2}\right)
\end{aligned} \qquad \text{for } m=1,\ldots,I_T \tag{35}
$$

The GDQ method applied to Eq. $(32)_3$ gives

$$
\begin{cases}
\sigma_{n(ij1)}=\bar{q}^{(-)}_{n(ij)}\,\text{(Boundary condition at the bottom surface of the shell)} \\
\displaystyle\sum_{k=1}^{I_T}\varsigma^{\zeta(1)}_{mk}\sigma_{n(ijk)}+\sigma_{n(ijm)}\left(\frac{1}{R_{1(ij)}+\zeta_m}+\frac{1}{R_{2(ij)}+\zeta_m}\right)=\frac{\sigma_{1(ijm)}}{R_{1(ij)}+\zeta_m}+\frac{\sigma_{2(ijm)}}{R_{2(ij)}+\zeta_m}+ \\
\displaystyle-\frac{1}{A_{1(ij)}\left(1+\zeta_m/R_{1(ij)}\right)}\left.\frac{\partial \bar{\tau}_{1n}}{\partial \alpha_1}\right|_{(ijm)}-\frac{\bar{\tau}_{1n(ijm)}}{A_{1(ij)}A_{2(ij)}\left(1+\zeta_m/R_{2(ij)}\right)}\left.\frac{\partial A_2}{\partial \alpha_1}\right|_{(ij)}+ \\
\displaystyle-\frac{1}{A_{2(ij)}\left(1+\zeta_m/R_{2(ij)}\right)}\left.\frac{\partial \bar{\tau}_{2n}}{\partial \alpha_2}\right|_{(ijm)}-\frac{\bar{\tau}_{2n(ijm)}}{A_{1(ij)}A_{2(ij)}\left(1+\zeta_m/R_{1(ij)}\right)}\left.\frac{\partial A_1}{\partial \alpha_2}\right|_{(ij)} \quad \text{for } m=2,\ldots,I_T
\end{cases} \tag{36}
$$

where derivatives $\frac{\partial \bar{\tau}_{1n}}{\partial \alpha_1},\frac{\partial \bar{\tau}_{2n}}{\partial \alpha_2}$ of the shear stresses $\bar{\tau}_{1n},\bar{\tau}_{2n}$ are approximated using the GDQ method. The boundary condition on the top surface of the shell, $\sigma_{n(ijT)}=\bar{q}^{(+)}_{n(ij)}$, is enforced by the following formula

$$
\bar{\sigma}_{n(ijm)}=\sigma_{n(ijm)}+\frac{\bar{q}^{(+)}_{n(ij)}-\sigma_{n(ijT)}}{h}\left(\zeta_m+\frac{h}{2}\right) \quad \text{for } m=1,\ldots,I_T \tag{37}
$$

We use the generalized Hooke's law [65,69,70] to evaluate the out-of-plane shear and normal strains $\gamma_{1n},\gamma_{2n},\varepsilon_n$ from

$$
\begin{aligned}
\gamma_{1n(ijm)} &= \frac{\overline{C}^{(m)}_{55}\bar{\tau}_{1n(ijm)}-\overline{C}^{(m)}_{45}\bar{\tau}_{2n(ijm)}}{\overline{C}^{(m)}_{55}\overline{C}^{(m)}_{44}-\left(\overline{C}^{(m)}_{45}\right)^2} \\
\gamma_{2n(ijm)} &= \frac{\overline{C}^{(m)}_{44}\bar{\tau}_{2n(ijm)}-\overline{C}^{(m)}_{45}\bar{\tau}_{1n(ijm)}}{\overline{C}^{(m)}_{55}\overline{C}^{(m)}_{44}-\left(\overline{C}^{(m)}_{45}\right)^2} \\
\varepsilon_{n(ijm)} &= \frac{\bar{\sigma}_{n(ijm)}-\overline{C}^{(m)}_{13}\varepsilon_{1(ijm)}-\overline{C}^{(m)}_{23}\varepsilon_{2(ijm)}-\overline{C}^{(m)}_{36}\gamma_{12(ijm)}}{\overline{C}^{(m)}_{33}}
\end{aligned} \tag{38}
$$

We note that relations (38) do not guarantee that the strain compatibility conditions are satisfied. Transverse strains computed using Eqs. (38) and in-plane strain components found from the displacements and strain–displacement relations can be used to further refine stresses $\sigma_1,\sigma_2,\tau_{12}$ as follows:

$$
\begin{aligned}
\bar{\sigma}_{1(ijm)} &= \overline{C}^{(m)}_{11}\varepsilon_{1(ijm)}+\overline{C}^{(m)}_{12}\varepsilon_{2(ijm)}+\overline{C}^{(m)}_{16}\gamma_{12(ijm)}+\overline{C}^{(m)}_{13}\varepsilon_{n(ijm)} \\
\bar{\sigma}_{2(ijm)} &= \overline{C}^{(m)}_{12}\varepsilon_{1(ijm)}+\overline{C}^{(m)}_{22}\varepsilon_{2(ijm)}+\overline{C}^{(m)}_{26}\gamma_{12(ijm)}+\overline{C}^{(m)}_{23}\varepsilon_{n(ijm)} \\
\bar{\tau}_{12(ijm)} &= \overline{C}^{(m)}_{16}\varepsilon_{1(ijm)}+\overline{C}^{(m)}_{26}\varepsilon_{2(ijm)}+\overline{C}^{(m)}_{66}\gamma_{12(ijm)}+\overline{C}^{(m)}_{36}\varepsilon_{n(ijm)}
\end{aligned} \tag{39}
$$

In summary the stress $(\bar{\sigma}_1,\bar{\sigma}_2,\bar{\tau}_{12},\bar{\tau}_{1n},\bar{\tau}_{2n},\bar{\sigma}_n)$ components in the 3-D shell are numerically computed using Eqs. (35), (37) and (39), whereas the strain $(\varepsilon_1,\varepsilon_2,\gamma_{12},\gamma_{1n},\gamma_{2n},\varepsilon_n)$ components are evaluated using the constitutive equations and Eqs. (38). It will be shown by several example problems that the present recovery approach gives their values close to those obtained using the FEM to analyze 3-D deformations of the shell.

6. Applications

Recalling that the accuracy and the stability of the GDQ method applied to laminated structures have been studied in [131–140], we focus here on providing results for through-the-thickness displacements, stresses and strains for sandwich shells. For all problems studied, a relatively fine 31×31 C–G–L grid in the mid-surface of the shell and 51 points along the transverse normal in each lamina for the recovery procedure are used. The numerical solution is found with the free software distributed by the authors [164].

Boundary conditions on the four edges of a shell are written in the sequence WSEN for West, South, East and North edges, respectively, and letters "C", "S" and "F" are used to identify clamped, simply-supported and traction free conditions. Thus, boundary conditions FCFC mean the West and the East edges are traction free and the South and the North edges are clamped. For a shell of revolution with the vertical line as the axis of symmetry, boundary conditions are described as CF on the South and the North surfaces. Geometries of doubly-curved free-form shells and panels investigated in this work are depicted in Fig. 1. The through-the-thickness distributions of volume fraction of the constituents used in the following examples are shown in Fig. 2. One of the constituents of the FGM is Zirconia for which, unless otherwise mentioned, Young's modulus E = 168 GPa and Poisson's ratio ν = 0.3.

In results presented in various Figures, symbols EDZ2, EDZ3 and EDZ4 are used. In these symbols, E indicates that an ESL theory is employed, D specifies that the governing equations are expressed in terms of the generalized displacements, Z stands for the Murakami function, and numbers 2, 3, 4 equal the value of $(N+1)$ in Eq. (11), e.g. see [148,160].

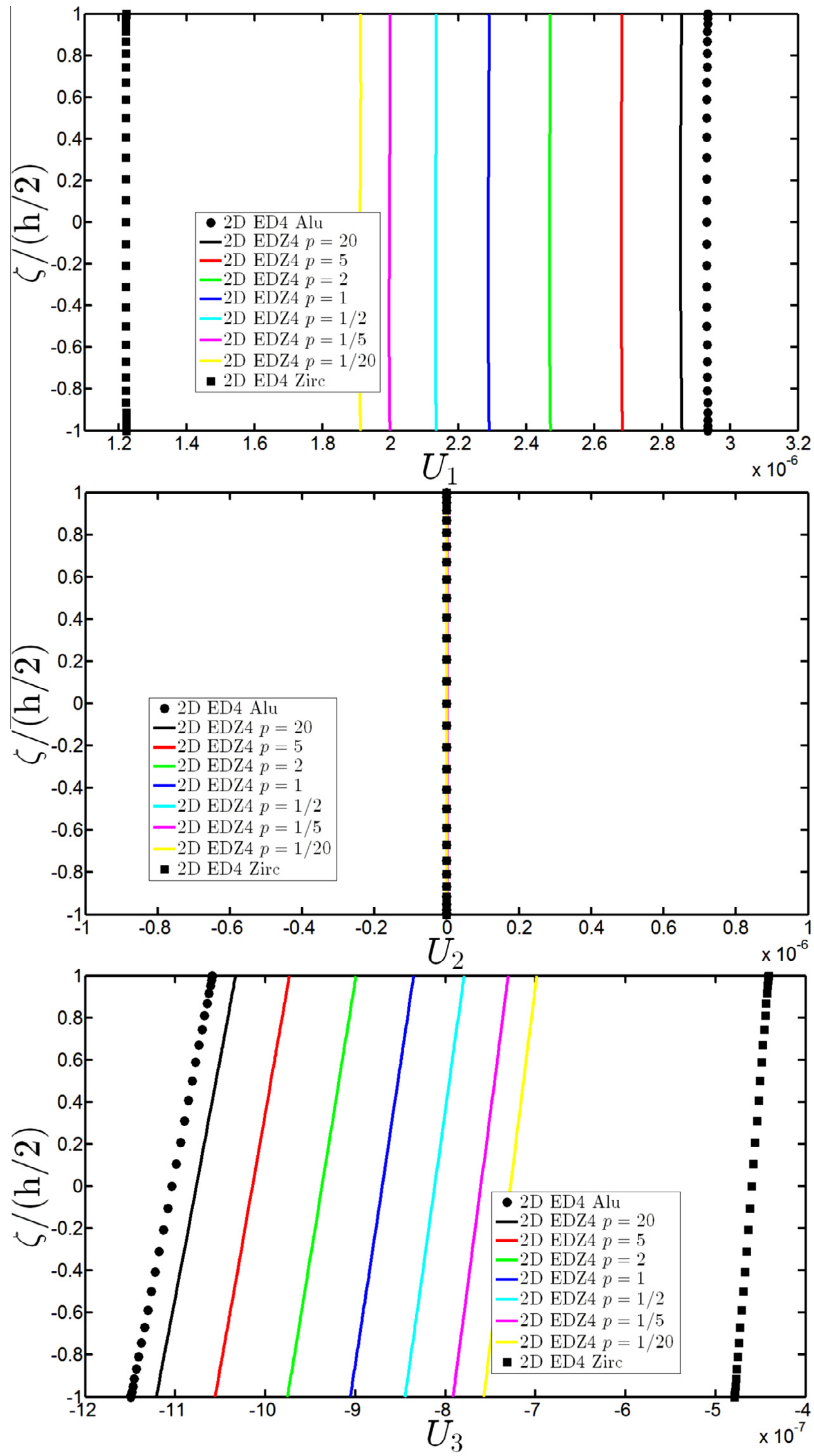

Fig. 13. Through-the-thickness variation of displacement components [m] for a CF free-form revolution shell of Fig. 1a at the point $A = (0.5(\alpha_1^1 - \alpha_1^0), 0.5(\alpha_2^1 - \alpha_2^0))$ with a $FGM^{M(MIX)}_{C(4P)(a^{(1)}=1/b^{(1)}=0/c^{(1)}/p^{(1)})}$/Aluminum/$FGM^{C(MIX)}_{M(4P)(a^{(3)}=1/b^{(3)}=0/c^{(3)}/p^{(3)})}$ lamination scheme, when uniformly distributed load $q_1^{(+)} = 10,000$ Pa is applied on the top surface, $h_1 = h_3 = 0.02$ m and $h_2 = 0.06$ m.

6.1. Comparison of present results with the analytical solution of Vel and Batra

In order to establish the validity of the posteriori recovery of the transverse shear and the transverse normal stresses for an FGM structure, we compare the presently computed results with the semi-analytical solution of Vel and Batra [5] who analyzed three dimensional (3D) deformations of FGM rectangular plates with the volume fraction of Aluminium ($E = 70$ GPa, $\nu = 0.3$) and Silicon Carbide ($E = 427$ GPa, $\nu = 0.17$) given by Eq. (5) and the Mori–Tanaka homogenization scheme. Results are presented in terms of the following nondimensionalized variables:

$$(\bar{u}_1, \bar{u}_2) = \frac{100 E_{Alu} h^2}{q_n^{(+)} L^3}(u_1, u_2), \quad \bar{u}_3 = \frac{100 E_{Alu} h^3}{q_n^{(+)} L^4} u_3$$
$$(\bar{\sigma}_x, \bar{\sigma}_y, \bar{\tau}_{xy}) = \frac{10h^2}{q_n^{(+)} L^2}(\sigma_x, \sigma_y, \tau_{xy}), \quad (\bar{\tau}_{xz}, \bar{\tau}_{yz}) = \frac{10h}{q_n^{(+)} L}(\tau_{xz}, \tau_{yz}), \quad \bar{\sigma}_z = \frac{\sigma_z}{q_n^{(+)}} \tag{40}$$

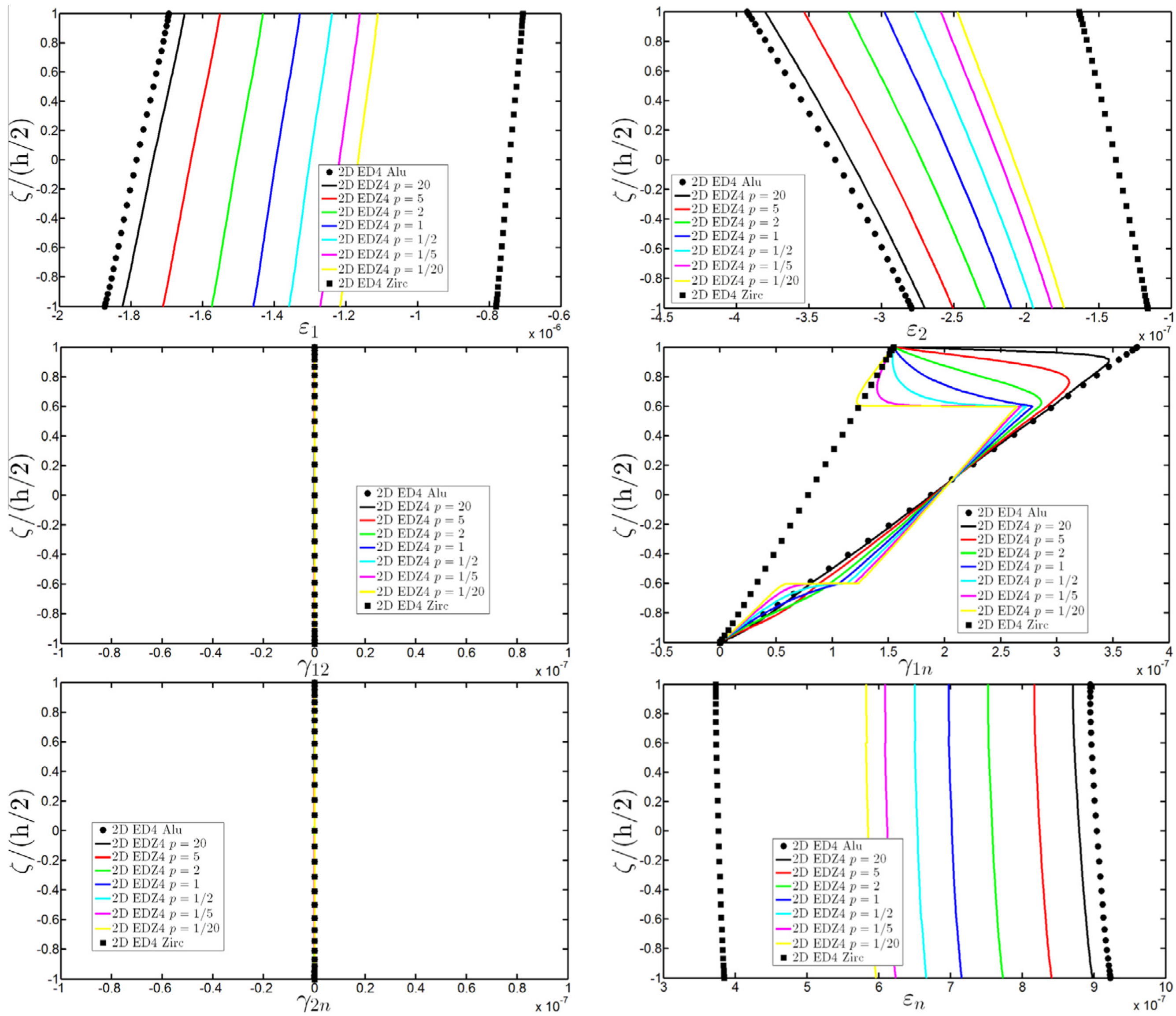

Fig. 14. Through-the-thickness variation of strains for a CF free-form revolution shell of Fig. 1a at the point $A = \left(0.5\left(\alpha_1^1 - \alpha_1^0\right), 0.5\left(\alpha_2^1 - \alpha_2^0\right)\right)$ with a $FGM^{M(MIX)}_{C(4P)(a^{(1)}=1/b^{(1)}=0/c^{(1)}/p^{(1)})}$/Aluminum/$FGM^{C(MIX)}_{M(4P)(a^{(3)}=1/b^{(3)}=0/c^{(3)}/p^{(3)})}$ lamination scheme, when uniformly distributed load $q_1^{(+)} = 10,000$ Pa is applied on the top surface, $h_1 = h_3 = 0.02$ m and $h_2 = 0.06$ m.

For an SSSS square plate of aspect ratio $L/h = 5$, with a sinusoidal load at the top surface $q_n^{(+)}, V_C^- = 0, V_C^+ = 0.75$ and $p = 2$, we have compared in Fig. 3 the presently computed values of $\bar{u}_3, \bar{\tau}_{xz}$ and $\bar{\sigma}_x$ using the ED3 and the ED4 theories with those of Ref. [5]. It is clear that the two sets of results are in excellent agreement with each other thereby verifying the accuracy of the present posterior stress recovery technique.

6.2. Flat laminated FG plates

Deformations of a flat sandwich rectangular $3 \times 3 \times 0.3$ m plate with $h_1 = h_3 = 7.5$ cm, $h_2 = 15$ cm, $q_n^{(+)} = -10$ MPa which is a particular case of a degenerate shell are studied with different ESL theories. In order to demonstrate the accuracy of the present stress recovery scheme for a sandwich structure with core material considerably softer than the material of the face sheets, results for sandwich plate made of homogeneous material are compared with those obtained by analyzing 3D deformations of the corresponding structures by the FEM using $20 \times 20 \times 12$ uniform 20-node brick elements. The Zirconia face sheets are perfectly bonded to the core made of an isotropic material having $E = 0.7$ GPa, $\nu = 0.3$; thus $E_1/E_2 = 240$. In order to account for both the effect of the thickness and the elastic modulus, we introduce a non-dimensional parameter $h_1E_1/h_2E_2 = \phi$. Thus for the sandwich plate being studied, $\phi = 120$. When either the core or the face sheet is made of an FGM, then the mean value of E is used to compute ϕ.

In Figs. 4–6 we have plotted through-the-thickness variations of the three components of displacements, and the six components of stresses and strains found using several higher-order ESL theories with and without the Murakami function (zigzag effect) along with those obtained by analyzing 3-D deformations of the sandwich structure with the core and the face sheets made of homogeneous materials with the FEM. It is clear that the zigzag effect is essential to capture deformations of the soft-core due to large differences in values of material parameters and thicknesses of the core and the face sheets. Furthermore, the EDZ4 gives the best accuracy among the four ESL theories considered but a good approximate solution is obtained using the EDZ2 and the EDZ3. We now use the EDZ3

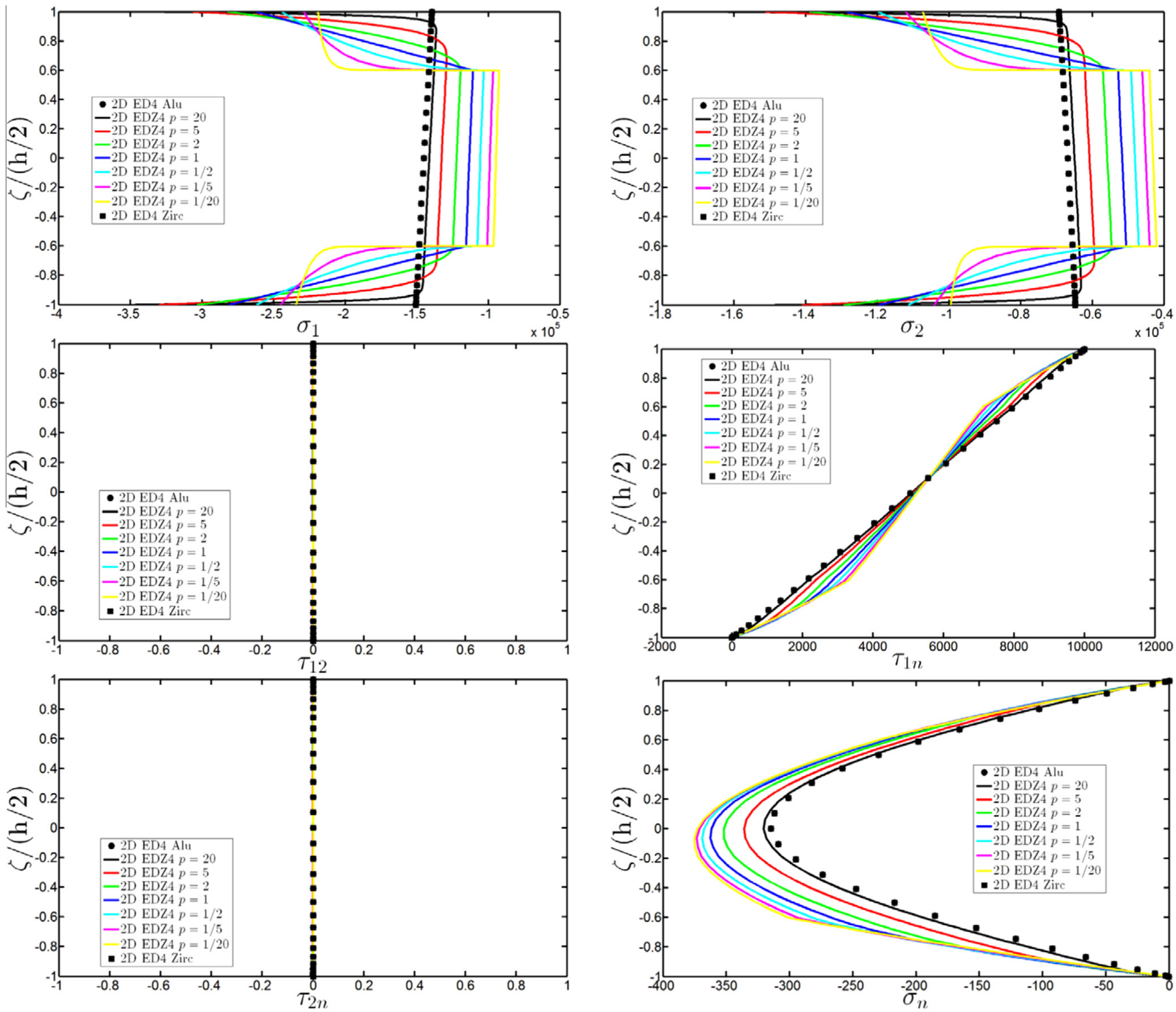

Fig. 15. Through-the-thickness variation of stresses [Pa] for a CF free-form revolution shell of Fig. 1a at the point $A = (0.5(\alpha_1^1 - \alpha_1^0), 0.5(\alpha_2^1 - \alpha_2^0))$ with a $FGM^{M(MIX)}_{C(4P)(a^{(1)}=1/b^{(1)}=0/c^{(1)}/p^{(1)})}$/Aluminum/$FGM^{C(MIX)}_{M(4P)(a^{(3)}=1/b^{(3)}=0/c^{(3)}/p^{(3)})}$ lamination scheme, when uniformly distributed load $q_1^{(+)} = 10{,}000$ Pa is applied on the top surface, $h_1 = h_3 = 0.02$ m and $h_2 = 0.06$ m.

to study deformations of the above sandwich plate except that $E = 0.35$ GPa for the core material and the face sheets are made of the FGM. For the $FGM^{M(MIX)}_{C(E)(a^{(1)}=10/b^{(1)})}$/ Core/$FGM^{C(MIX)}_{M(E)(a^{(3)}=10/b^{(3)})}$ plate the through-the-thickness variation of the volume fraction of the ceramic is assumed to be given by Eq. (3) and is depicted in Fig. 2a for $a^{(1)} = a^{(3)} = a = 10$ and $b^{(1)} = b^{(3)} = b = 1/20, 1/2, 1, 2, 20$. For comparison, the 3-D deformations of the Zirconia/Core/Zirconia ($\phi = 120$) plate made of isotropic and homogeneous materials are analyzed by using $20 \times 20 \times 12$ 20-node brick elements with the Strand 7 software. Values of the parameter ϕ are summarized in Table 1 (case a) with respect to the values of E of the top and the bottom face sheets of the sandwich plate. Note that for most of the cases studied, due to the mixing of the Zirconia with the softer material, $\phi < 1$. The through-the-thickness variation of the displacements, stresses and strains depicted in Figs. 7–9 reveal that the results from the EDZ3 and the 3-D elasticity theory are virtually identical to each other. For the face sheets made of the FGM, results for $b = 1/20$ and 20 are quantitatively quite different from those for other values of b but results for the five values of b considered are qualitatively similar to each other. Even though the transverse shear stresses and strains in the core are nearly uniform, their values strongly depend upon the value of b.

6.3. Doubly-curved laminated FG panels

We study deformations of a doubly curved FCFF sandwich panel with equal principal radii $R_1 = R_2 = R = 1$ m, $h = 0.1$ m, $h_1 = h_3 = 0.015$ m, $h_2 = 0.07$ m, and subjected to a uniform pressure, $p_n^{(+)} = -10$ MPa, on the top layer. For comparison, the 3-D deformations of geometrically identical Zirconia/Core/Zirconia sandwich structure with $E = 3.5$ GPa, $\nu = 0.3$ for the core material and using 25,600 ($40 \times 40 \times 16$) 20 node brick elements were analyzed by the FEM. The non-dimensional parameter $\phi \simeq 10.3$ for this structure. We now assume that it can be modeled as a three layered structure by modifying the definition of two plies. This can be achieved by the Weibull distribution shown in Fig. 2b. The two plies are 5 cm thick but the effective sheets and the core have a variable thickness which depends on the volume fraction parameters. Thus the lamination

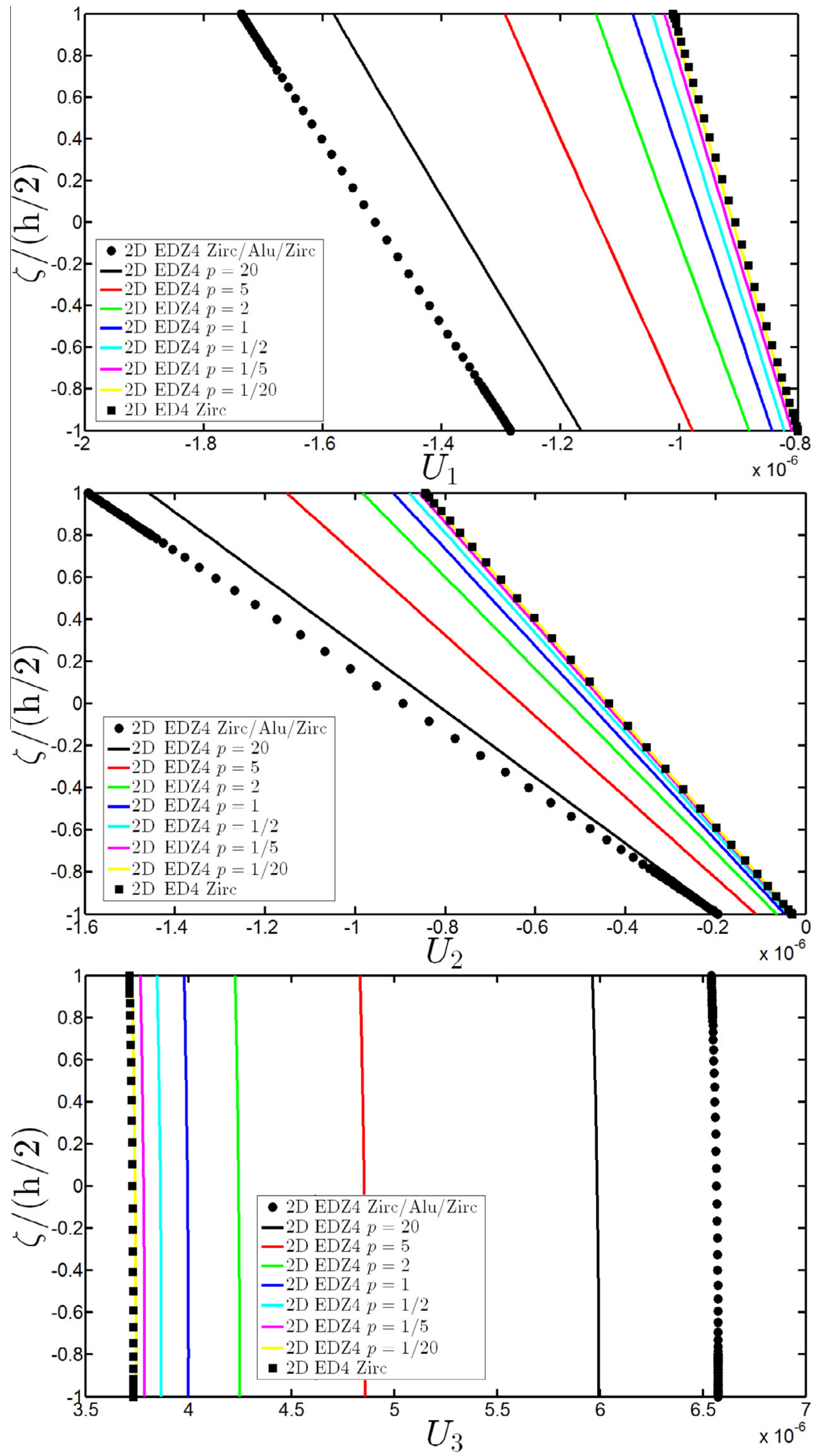

Fig. 16. Through-the-thickness variation of displacement components [m] for a CFFC free-form revolution panel of Fig. 1b at the point $C = \left(0.25\left(\alpha_1^1 - \alpha_1^0\right), 0.25\left(\alpha_2^1 - \alpha_2^0\right)\right)$ with a Zirconia/$FGM^{M(MIX)}_{C(4P)(a^{(2)}=1/b^{(2)}=1/c^{(2)}=2/p^{(2)})}$/Zirconia lamination scheme, when uniformly distributed load $q_n^{(+)} = -10,000$ Pa is applied on the top surface, $h_1 = h_3 = 0.01$ m and $h_2 = 0.08$ m.

scheme is given by $FGM^{M(MIX)}_{C(W)(a^{(1)}/b^{(1)}=50)}/FGM^{C(MIX)}_{M(W)(a^{(2)}/b^{(2)}=50)}$. Note that the FEM solution of 3D deformations of the Zirconia/Core/Zirconia sandwich structure using $h_1 = h_3 = 0.015$ m and $h_2 = 0.07$ m is also displayed. It can be used as a reference since the other thicknesses of the FG lamination schemes vary with the volume fractions. It is clear from results plotted in Figs. 10–12 that values of parameters $a^{(1)}$, $a^{(2)}$ significantly affect through-the-thickness distributions of displacements, stresses and strains. The maximum values of the in-plane normal stresses and the maximum value of the out-of-plane strains in the core are reduced by changing the parameter $a^{(1)}$ as 0.3, 0.4, 0.5, 0.6, 0.7, 0.8 and inversely $a^{(2)}$ as 0.8, 0.7, 0.6, 0.5, 0.4, 0.3. The values of the non-dimensional fictitious parameter $\tilde{\phi}$ for the different values of the volume fractions are given in Table 1 (case b). Note that the mean values of the elastic moduli are not

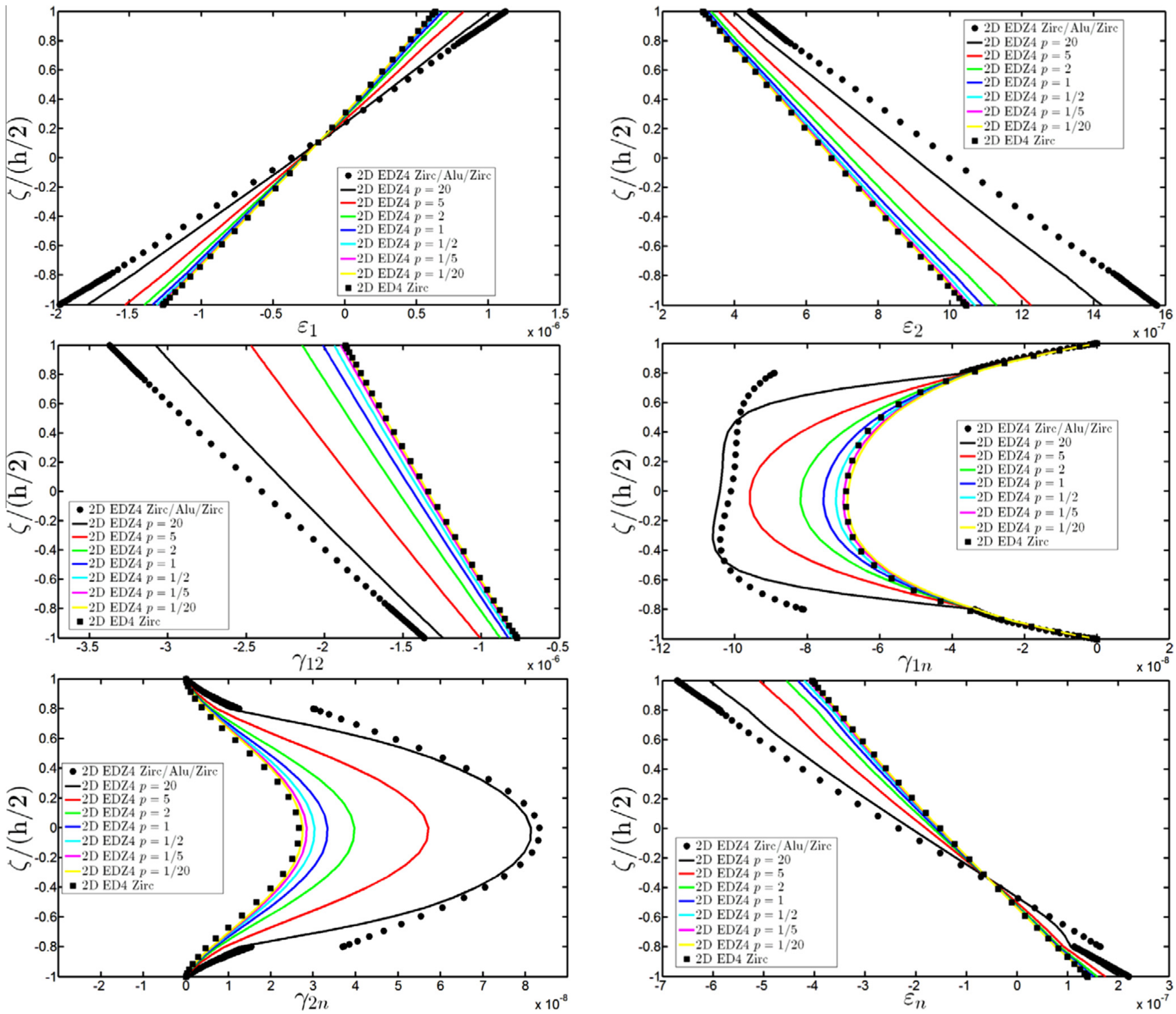

Fig. 17. Through-the-thickness variation of strains for a CFFC free-form revolution panel of Fig. 1b at the point $C = \left(0.25\left(\alpha_1^1 - \alpha_1^0\right), 0.25\left(\alpha_2^1 - \alpha_2^0\right)\right)$ with a Zirconia/$FGM^{M(MIX)}_{C(4P)(a^{(2)}=1/b^{(2)}=1/c^{(2)}=2/p^{(2)})}$/Zirconia lamination scheme, when uniformly distributed load $q_n^{(+)} = -10,000$ Pa is applied on the top surface, $h_1 = h_3 = 0.01$ m and $h_2 = 0.08$ m.

considered for the present calculations, whereas the elastic moduli of the Zirconia and the Aluminum are used with the following fictitious sheets and core thicknesses denoted by subscripts s and c, respectively: $h_s = 0.015$ m, $h_c = 0.035$ m; $h_s = 0.02$ m, $h_c = 0.03$ m; $h_s = 0.025$ m, $h_c = 0.025$ m; $h_s = 0.03$ m, $h_c = 0.020$ m; $h_s = 0.035$ m, $h_c = 0.015$ m; $h_s = 0.04$ m, $h_c = 0.01$ m.

6.4. Free-form doubly-curved laminated FG shells

The first example is the CF $FGM^{M(MIX)}_{C(4P)(a^{(1)}=1/b^{(1)}=0/c^{(1)}/p^{(1)})}$/aluminum/$FGM^{C(MIX)}_{M(4P)(a^{(3)}=1/b^{(3)}=0/c^{(3)}/p^{(3)})}$ shell of revolution (Fig. 2a) with a free-form meridian generated by the Bézier curve with $\bar{\mathbf{x}}_1 = [2\ 1.2\ 0.85\ 0.75\ 0.7], \bar{\mathbf{x}}'_3 = [0\ 0.3\ 1\ 1.5\ 2], \mathbf{w} = [1\ 1\ 1\ 1\ 1]$, $R_b = 0$ m, $h = 0.1$ m and $\vartheta_0 = 2\pi$, and a tangential force $p_1^{(+)} = 10$ MPa applied at the top surface of the shell. The through-the-thickness variation of the volume fraction of the constituents is shown in Fig. 2c, and values of material parameters for the aluminum are $E = 70$ GPa, $\nu = 0.3$ and those for the ceramic (Zirconia) are listed above. The results of the recovered displacements, strains and stresses on the transverse normal passing through the point $A = \left(0.5\left(\alpha_1^1 - \alpha_1^0\right), 0.5\left(\alpha_2^1 - \alpha_2^0\right)\right)$ for the power law exponent $p^{(1)} = p^{(3)} = p$ varying from 20 (FGM almost all Aluminum) to 1/20 (FGM almost all Zirconia) are shown in Figs. 13–15. Whereas the ED4 is used for two isotropic cases (structure made of Aluminum and Zirconia), the EDZ4 is used for other values of p. As has been shown by numerous investigators for flat plates, results for the FGM materials are in-between those for homogeneous structures made of pure Aluminum and Zirconia. The values of the non-dimensional parameter ϕ for the FGMs are reported in Table 1 (case c), considering the mean values of the elastic moduli of the two face sheets. For all FGMs studied in this example problem, ϕ varies between 0.395 and 0.764.

The second example is a CFFC Zirconia/$FGM^{M(MIX)}_{C(4P)(a^{(1)}=1/b^{(1)}=1/c^{(1)}=2/p^{(1)})}$/Zirconia shell of revolution, similar to that shown in Fig. 2d but with different thicknesses of the core and the face sheets. It is formed by the Bézier geometric parameters $\bar{\mathbf{x}}_1 = [0.8\ 1.3\ 1.5\ 1.4\ 1.2], \bar{\mathbf{x}}'_3 = [0\ 0.5\ 1\ 1.5\ 2], \mathbf{w} = [1\ 1\ 1\ 1\ 1]$, $R_b = 0$ m, $h = 0.1$ m and $\vartheta_0 = 2\pi/3$, and a normal pressure

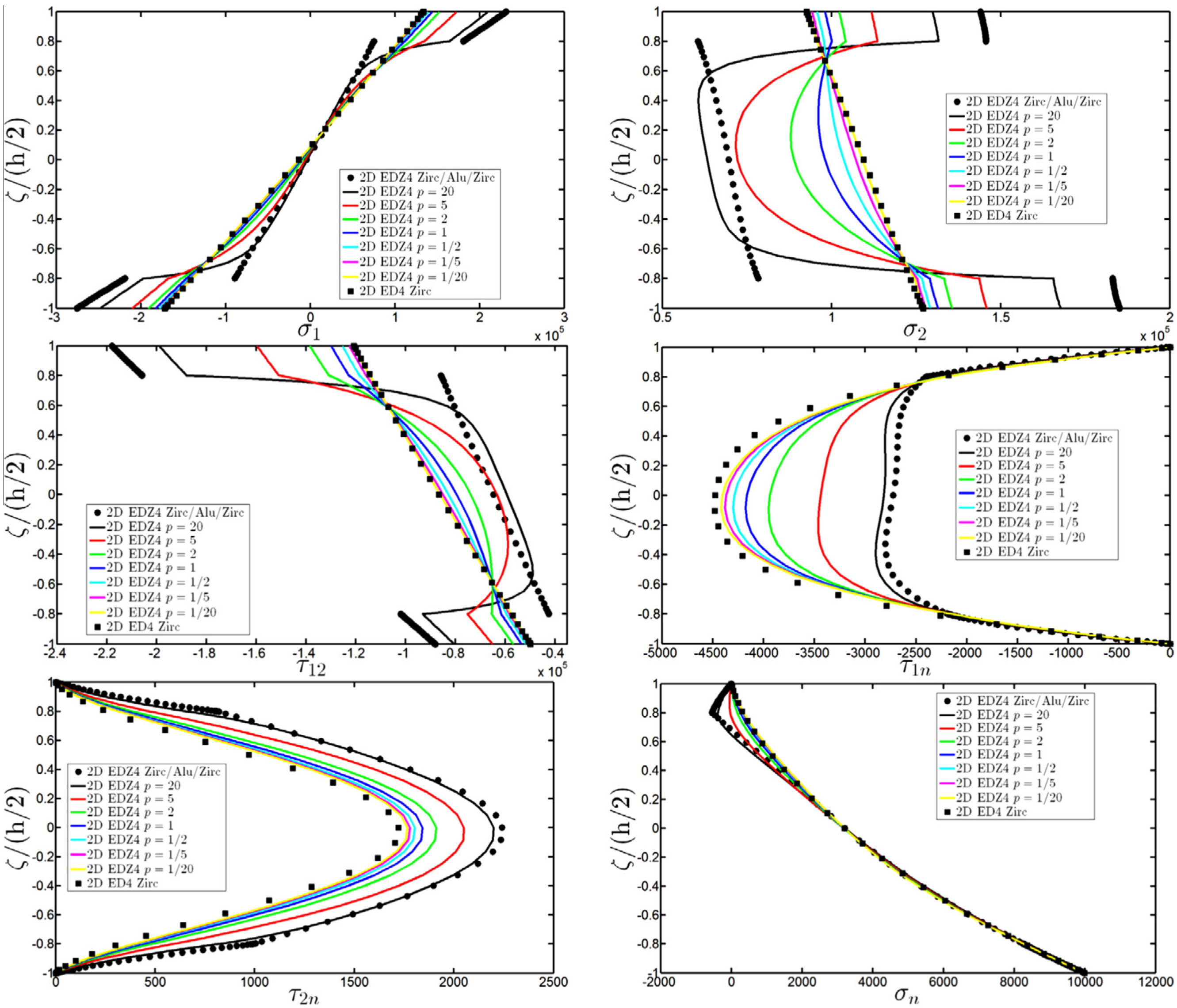

Fig. 18. Through-the-thickness variation of stresses for a CFFC free-form revolution panel of Fig. 1b at the point $C = (0.25(\alpha_1^1 - \alpha_1^0), 0.25(\alpha_2^1 - \alpha_2^0))$ with a Zirconia/$FGM^{M(MIX)}_{C(4P)(a^{(2)}=1/b^{(2)}=1/c^{(2)}=2/p^{(2)})}$/Zirconia lamination scheme, when uniformly distributed load $q_n^{(+)} = -10{,}000$ Pa is applied on the top surface, $h_1 = h_3 = 0.01$ m and $h_2 = 0.08$ m.

$p_n^{(+)} = -10$ MPa applied on the top surface. The two constituent materials are Zirconia and Aluminum, and the thickness of the top and the bottom face sheets and of the core are $h_1 = h_3 = 0.01$ m, $h_2 = 0.08$ m. Results on the transverse normal through the point $C = (0.25(\alpha_1^1 - \alpha_1^0), 0.25(\alpha_2^1 - \alpha_2^0))$ presented in Figs. 16–18 reveal that stresses for the FGM structures are in-between those for the two limiting cases, namely those for the structures made of pure Zirconia and pure Aluminum. Values of ϕ listed in Table 1 (case d) vary between 0.13 and 0.43.

7. Conclusions

Several aspects related to the static analysis of FG laminated free-form shells and doubly-curved shells have been studied by using equivalent single layer (ESL) theories of different orders. The differential equations of the ESL theory are numerically solved by using the Generalized Differential Quadrature (GDQ) method. Through-the-thickness variations of stresses, strains and displacements computed by using an iterative a posteriori stress recovery technique are found to be close to those obtained by solving the 3-D equations of linear elasticity. Furthermore, their values for structures made of FGMs are in-between those for the same structures made of homogeneous materials with material properties of the two constituents of the FGM. When both FGMs and Bézier curves are considered, the designer can tailor both the mechanical and the geometric properties of the structure under study to optimize their performance.

Acknowledgments

The research topic is one of the subjects of the Centre of Study and Research for the Identification of Materials and Structures (CIMEST) –"M. Capurso" of the University of Bologna (Italy). RCB's work was partially supported by the US Office of Naval Research Grant N00014-11-1-0594 to Virginia Polytechnic Institute and State University with Dr. Y.D.S. Rajapakse as the Program Manager.

References

[1] Shen HS. Functionally graded materials. Nonlinear analysis of plates and shells. CRC Press; 2009.
[2] Cheng Z-Q, Batra RC. Deflection relationships between the homogeneous plate theory and different functionally graded plate theories. Arch Mech 2000;52:143–58.
[3] Yang J, Shen H-S. Nonlinear bending analysis of shear deformable functionally graded plates subjected to thermo-mechanical loads under various boundary conditions. Compos Part B Eng 2003;34:103–15.
[4] Batra RC. Torsion of a functionally graded cylinder. AIAA J 2006;44:1363–5.
[5] Vel SS, Batra RC. Exact solutions for thermoelastic deformations of functionally graded thick rectangular plates. AIAA J 2002;40:1421–33.
[6] Vel SS, Batra RC. Three-dimensional exact solution for the vibration of functionally graded rectangular plates. J Sound Vib 2004;272:703–30.
[7] Vel SS, Batra RC. Three-dimensional analysis of transient thermal stresses in functionally graded plates. Int J Solids Struct 2004;40:7181–96.
[8] Efraim E, Eisenberger M. Exact vibration analysis of variable thickness thick annular isotropic and FGM plates. J Sound Vib 2007;299:720–38.
[9] Tornabene F. Free vibration analysis of functionally graded conical, cylindrical and annular shell structures with a four-parameter power-law distribution. Comput Methods Appl Mech Eng 2009;198:2911–35.
[10] Tornabene F, Viola E. Free vibrations of four-parameter functionally graded parabolic panels and shell of revolution. Eur J Mech A-Solid 2009;28: 991–1013.
[11] Tornabene F, Viola E. Free vibration analysis of functionally graded panels and shells of revolution. Meccanica 2009;44:255–81.
[12] Tornabene F, Viola E, Inman DJ. 2-D differential quadrature solution for vibration analysis of functionally graded conical, cylindrical and annular shell structures. J Sound Vib 2009;328:259–90.
[13] Viola E, Tornabene F. Free vibrations of three parameter functionally graded parabolic panels of revolution. Mech Res Commun 2009;36:587–94.
[14] Li S-R, Hua X, Batra RC. Free vibration of 3-layer circular cylindrical shells with functionally graded middle layer. Mech Res Commun 2010;37:577–80.
[15] Hosseini-Hashemi Sh, Ilkhani MR, Fadaee M. Accurate natural frequencies and critical speeds of a rotating functionally graded moderately thick cylindrical shell. Int J Mech Sci 2013;76:9–20.
[16] Tornabene F, Liverani A, Caligiana G. FGM and laminated doubly-curved shells and panels of revolution with a free-form meridian: a 2-D GDQ solution for free vibrations. Int J Mech Sci 2011;53:446–70.
[17] Viola E, Rossetti L, Fantuzzi N. Numerical investigation of functionally graded cylindrical shells and panels using the generalized unconstrained third order theory coupled with the stress recovery. Compos Struct 2012:3736–58.
[18] Fereidoon A, Mohyeddin A, Sheikhi M, Rahmani H. Bending analysis of functionally graded annular sector plates by extended Kantorovich method. Compos Part B Eng 2012;43:2172–9.
[19] Setoodeh AR, Tahani M, Selahi E. Transient dynamic and free vibration analysis of functionally graded truncated conical shells with non-uniform thickness subjected to mechanical shock loading. Compos Part B Eng 2012;43:2161–71.
[20] Tornabene F, Ceruti A. Mixed static and dynamic optimization of four-parameter functionally graded completely doubly-curved and degenerate shells and panels using GDQ method. Math Prob Eng 2013;2013:1–33. Article ID 867079.
[21] Viola E, Rossetti L, Fantuzzi N, Tornabene F. Static analysis of functionally graded conical shells and panels using the generalized unconstrained third order theory coupled with the stress recovery. Compos Struct 2014;112: 44–65.
[22] Su Z, Jin G, Shi S, Ye T, Jia X. A unified solution for vibration analysis of functionally graded cylindrical, conical shells and annular plates with general boundary conditions. Int J Mech Sci 2014;80:62–80.
[23] Carrera E, Brischetto S, Cinefra M, Soave M. Effects of thickness stretching in functionally graded plates and shells. Compos Part B: Eng 2011;42:123–33.
[24] Liew KM, Zhao X, Ferreira AJM. A review of meshless methods for laminated and functionally graded plates and shells. Compos Struct 2011;93:2031–41.
[25] Dozio L. Exact free vibration analysis of Lévy FGM plates with higher-order shear and normal deformation theories. Compos Struct 2014;111:415–25.
[26] Hong CC. Thermal vibration of magnetostrictive functionally graded material Shells by considering the varied effects of shear correction coefficient. Int J Mech Sci 2014;85:20–9.
[27] Sofiyev AH. On the dynamic buckling of truncated conical shells with functionally graded coatings subject to a time dependent axial load in the large deformation. Compos Part B: Eng 2014;58:524–33.
[28] Sofiyev AH, Kuruoglu N. Buckling and vibration of shear deformable functionally graded orthotropic cylindrical shells under external pressures. Thin-Walled Struct 2014;78:121–30.
[29] Abrate S. Free vibration, buckling, and static deflections of functionally graded plates. Compos Sci Technol 2006;66:2383–94.
[30] Abrate S. Functionally graded plates behave like homogeneous plates. Compos Part B: Eng 2008;39:151–8.
[31] Qian LF, Batra RC, Chen LM. Analysis of cylindrical bending thermoelastic deformations of functionally graded plates by a meshless local Petrov–Galerkin method. Comput Mech 2004;33:263–73.
[32] Qian LF, Batra RC, Chen LM. Static and dynamic deformations of thick functionally graded elastic plate by using higher-order shear and normal deformable plate theory and meshless local Petrov–Galerkin method. Compos Part B Eng 2004;35:685–97.
[33] Gilhooley DF, Batra RC, Xiao JR, Mc Carthy MA, Gillespie Jr JW. Analysis of thick functionally graded plates by using higher-order shear and normal deformable plate theory and MLPG method with radial basis functions. Compos Struct 2007;80:539–52.
[34] Batra RC, Vidoli S. Higher order piezoelectric plate theory derived from a three-dimensional variational principle. AIAA J 2002;40:91–104.
[35] Ye T, Jin G, Shi S, Ma X. Three-dimensional free vibration analysis of thick cylindrical shells with general end conditions and resting on elastic foundations. Int J Mech Sci 2014;84:120–37.
[36] Ke LL, Yang J, Kitipornchai S, Bradford MA, Wang YS. Axisymmetric nonlinear free vibration of size-dependent functionally graded annular microplates. Compos Part B Eng 2013;53:207–17.
[37] Joodaky A, Joodaky I, Hedayati M, Masoomi R, Farahani EB. Deflection and stress analysis of thin FGM skew plates on Winkler foundation with various boundary conditions using extended Kantorovich method. Compos Part B Eng 2013;51:191–6.
[38] Qu Y, Long X, Yuan G, Meng G. A unified formulation for vibration analysis of functionally graded shells of revolution with arbitrary boundary conditions. Compos Part B Eng 2013;50:381–402.
[39] Mori T, Tanaka K. Average stress in matrix and average elastic energy of materials with misfitting inclusions. Acta Metal 1973;21:571–4.
[40] Mura T. Micromechanics of defects in solids. The Hague: Martinus Nijhoff; 1982.
[41] Hashin Z. Analysis of composite materials – A survey. J Appl Mech 1983;50:481–505.
[42] Benveniste Y. A new approach to the application of Mori–Tanaka's theory in composite materials. Mech Mat 1987;6:147–57.
[43] Timoshenko S, Woinowsky-Krieger S. Theory of plates and shells. McGraw-Hill; 1959.
[44] Flügge W. Stresses in shells. Springer-Verlag; 1960.
[45] Gol'denveizer AL. Theory of elastic thin shells. Pergamon Press; 1961.
[46] Novozhilov VV. Thin shell theory. P. Noordhoff; 1964.
[47] Ambartusumyan SA, Theory of anisotropic shells, NASA-TT-F-118; 1964.
[48] Kraus H. Thin elastic shells. John Wiley & Sons; 1967.
[49] Lekhnitskii SG, Tsai SW, Cheron T. Anisotropic plates, gordon and breach. Science Publishers; 1968.
[50] Leissa AW, Vibration of plates, NASA-SP-160; 1969.
[51] Leissa AW, Vibration of shells, NASA-SP-288; 1973.
[52] Saada AS. Elasticity, theory and applications. Pergamon Press; 1974.
[53] Szilard R. Theory and analysis of plates. Prentice-Hall; 1974.
[54] Donnel LH. Beams, plates and shells. McGraw-Hill; 1976.
[55] Lekhnitskii SG. Theory of elasticity of an anisotropic body. Mir Publishers; 1981.
[56] Calladine CR. Theory of shell structures. Cambridge University Press; 1983.
[57] Gould PL. Finite element analysis of shells of revolution. Pitman Publishing; 1985.
[58] Niordson FI. Shell theory. North-Holland; 1985.
[59] Markuš Š. The mechanics of vibrations of cylindrical shells. Elsevier; 1988.
[60] Tzou HS. Piezoelectric shells. Kluwer Academic Publishers; 1993.
[61] Rogacheva NN. The theory of piezoelectric shells and plates. CRC Press; 1994.
[62] Kaw AK. Mechanics of composite materials. CRC Press; 1997.
[63] Libai A, Simmonds JG. The nonlinear theory of elastic shells. Cambridge University Press; 1998.
[64] Gould PL. Analysis of shells and plates. Prentice-Hall; 1999.
[65] Reddy JN. Theory and analysis of elastic plates. Taylor & Francis; 1999.
[66] Vorovich II. Nonlinear theory of shallow shells. Springer; 1999.
[67] Ciarlet P. Theory of shells. Elsevier; 2000.
[68] Ventsel E, Krauthammer T. Thin plates and shells. Marcel Dekker; 2001.
[69] Reddy JN. Energy principles and variational methods in applied mechanics. John Wiley & Sons; 2002.
[70] Reddy JN. Mechanics of laminated composite plates and shells. CRC Press; 2003.
[71] Wempner G, Talaslidis D. Mechanics of solids and shells. CRC Press; 2003.
[72] Qatu MS. Vibration of laminated shells and plates. Elsevier; 2004.
[73] Soedel W. Vibrations of shells and plates. Marcel Dekker; 2004.
[74] Vinson JR, Sierakowski RL. The behavior of structures composed of composite materials. Kluwer Academic Publishers.; 2004.
[75] Carrera E, Brischetto S, Nali P. Plates and shells for smart structures. John Wiley & Sons; 2011.
[76] Chapelle D, Bathe KJ. The finite element analysis of shells – fundamentals. Springer; 2011.
[77] Leissa AW, Qatu MS. Vibrations of continuous systems. McGraw-Hill; 2011.
[78] Calvi GM, Nascimbene R. Progettere i Gusci. IUSS Press; 2011.
[79] Tornabene F, Meccanica delle Strutture a Guscio in Materiale Composito. Il Metodo Generalizzato di Quadratura Differenziale, Esculapio; 2012.
[80] Tornabene F, Fantuzzi N, Mechanics of laminated composite doubly-curved shell structures. The generalized differential quadrature method and the strong formulation finite element method, Esculapio; 2014.
[81] Yang JS, Batra RC. Thickness shear vibrations of a circular cylindrical piezoelectric shell. J Acoust Soc Am 1995;97:309–12.
[82] Carrera E. Multilayered shell theories accounting for layerwise mixed description, part 1: governing equations. AIAA J 1999;37:1107–16.
[83] Carrera E. Multilayered shell theories accounting for layerwise mixed description, part 2: numerical evaluations. AIAA J 1999;37:1117–24.

[84] Carrera E. Historical review of zig-zag theories for multilayered plates and shells. Appl Mech Rev 2003;56:287–308.
[85] Cho M, Kim KO, Kim MH. Efficient higher-order shell theory for laminated composites. Compos Struct 1996;34:197–212.
[86] Lo KH, Christensen RM, Wu EM. A high-order theory of plate deformation – part 1: homogeneous plates. J Appl Mech 1977;44:663–8.
[87] Vel SS, Batra RC. Analytical solutions for rectangular thick laminated plates subjected to arbitrary boundary conditions. AIAA J 1999;37:1464–73.
[88] Vel SS, Batra RC. The generalized plane strain deformations of thick anisotropic composite laminated plates. Int J Solids Struct 2000;37:715–33.
[89] Vel SS, Batra RC. Closure to the generalized plane strain deformations of thick anisotropic composite laminated plates. Int J Solids Struct 2000;38:483–9.
[90] Efraim E, Eisenberger M. Exact vibration frequencies of segmented axisymmetric shells. Thin-Walled Struct 2006;44:281–9.
[91] Efraim E, Eisenberger M. Dynamic stiffness vibration analysis of thick spherical segments with variable thickness. J Mech Mat Struct 2010;5: 821–35.
[92] Qatu MS, Sullivan RW, Wang W. Recent research advances on the dynamic analysis of composite shells: 2000–2009. Compos Struct 2011;93:14–31.
[93] Asadi E, Wang W, Qatu MS. Static and vibration analyses of thick deep laminated cylindrical shells using 3D and various shear deformation theories. Compos Struct 2012;94:494–500.
[94] Liu B, Xing YF, Qatu MS, Ferreira AJM. Exact characteristic equations for free vibrations of thin orthotropic circular cylindrical shells. Compos Struct 2012;94:484–93.
[95] Maleki S, Tahani M. Non-linear analysis of fiber-reinforced open conical shell panels considering variation of thickness and fiber orientation under thermo-mechanical loadings. Compos Part B Eng 2013;52:245–61.
[96] Nascimbene R. Towards non-standard numerical modeling of thin-shell structures: geometrically linear formulation. Int J Comput Methods Eng Sci Mech 2014;15:126–41.
[97] Fazzolari FA, Banerjee JR. Axiomatic/asymptotic PVD/RMVT-based shell theories for free vibrations of anisotropic shells using an advanced Ritz formulation and accurate curvature descriptions. Compos Struct 2014;108: 91–110.
[98] Jin G, Ye T, Jia X, Gao S. A general Fourier solution for the vibration analysis of composite laminated structure elements of revolution with general elastic restraints. Compos Struct 2014;109(1):150–68.
[99] Jin G, Ye T, Ma X, Chen Y, Su Z, Xie X. A unified approach for the vibration analysis of moderately thick composite laminated cylindrical shells with arbitrary boundary conditions. Int J Mech Sci 2013;75:357–76.
[100] Qu Y, Long X, Wu S, Meng G. A unified formulation for vibration analysis of composite laminated shells of revolution including shear deformation and rotary inertia. Compos Struct 2013;98:169–91.
[101] Panda HS, Sahu SK, Parhi PK. Effects of moisture on the frequencies of vibration of woven fibre composite doubly curved panels with strip delaminations. Thin Wall Struct 2014;78:79–86.
[102] Sofiyev AH, Kuruoglu N. Buckling and vibration of shear deformable functionally graded orthotropic cylindrical shells under external pressures. Thin Wall Struct 2014;78:121–30.
[103] Belabed Z, Ahmed Houari MS, Tounsi A, Mahmoud SR, Anwar Bég O. An efficient and simple higher order shear and normal deformation theory for functionally graded material (FGM) plates. Compos Part B Eng 2014;60:274–83.
[104] Jin G, Ye T, Jia X, Gao S. A general Fourier solution for the vibration analysis of composite laminated structure elements of revolution with general elastic restraints. Compos Struct 2014;109(1):150–68.
[105] Qu Y, Meng G. Dynamic analysis of composite laminated and sandwich hollow bodies of revolution based on three-dimensional elasticity theory. Compos Struct 2014;112:378–96.
[106] Sofiyev AH. The influence of non-homogeneity on the frequency-amplitude characteristics of laminated orthotropic truncated conical shell. Compos Struct 2014;107:334–45.
[107] Su Z, Jin G, Shi S, Ye T. A unified accurate solution for vibration analysis of arbitrary functionally graded spherical shell segments with general end restraints. Compos Struct 2014;111:271–84.
[108] Groh RMJ, Weaver PM. Buckling analysis of variable angle tow, variable thickness panels with transverse shear effects. Compos Struct 2014;107: 482–93.
[109] Ye T, Jin G, Chen Y, Ma X, Su Z. Free vibration analysis of laminated composite shallow shells with general elastic boundaries. Compos Struct 2013;106: 470–90.
[110] Jahromi HN, Aghdam MM, Fallah A. Free vibration analysis of Mindlin plates partially resting on Pasternak foundation. Int J Mech Sci 2013;75:1–7.
[111] Qu Y, Long X, Li H, Meng G. A variational formulation for dynamic analysis of composite laminated beams based on a general higher-order shear deformation theory. Compos Struct 2013;102:175–92.
[112] Qu Y, Long X, Yuan G, Meng G. A unified formulation for vibration analysis of functionally graded shells of revolution with arbitrary boundary conditions. Compos Part B Eng 2013;50:381–402.
[113] Li Z-M, Qiao P. On an exact bending curvature model for nonlinear free vibration analysis shear deformable anisotropic laminated beams. Compos Struct 2013;108:243–58.
[114] Fazzolari FA. A refined dynamic stiffness element for free vibration analysis of cross-ply laminated composite cylindrical and spherical shallow shells. Compos Part B Eng 2014;62:143–58.
[115] Sofiyev AH. The combined influences of heterogeneity and elastic foundations on the nonlinear vibration of orthotropic truncated conical shells. Compos Part B Eng 2014;61:324–39.
[116] Duc ND, Quan TQ. Transient responses of functionally graded double curved shallow shells with temperature-dependent material properties in thermal environment. Eur J Mech A/Solids 2014;47:101–23.
[117] Phung-Van P, Nguyen-Thoi T, Dang-Trung H, Nguyen-Minh N. A cell-based smoothed discrete shear gap method (CS-FEM-DSG3) using layerwise theory based on the C0-HSDT for analyses of composite plates. Compos Struct 2014;111:553–65.
[118] Shu C. Differential quadrature and its application in engineering. Springer; 2000.
[119] Bellman R, Casti J. Differential quadrature and long-term integration. J Math Anal Appl 1971;34:235–8.
[120] Bert C, Malik M. Differential quadrature method in computational mechanics. Appl Mech Rev 1996;49:1–27.
[121] Striz AG, Chen WL, Bert CW. Static analysis of structures by the quadrature element method (QEM). Int J Solids Struct 1994;31:2807–18.
[122] Striz AG, Chen WL, Bert CW. Free vibration of plates by the high accuracy element method. J Sound Vib 1997;202:689–702.
[123] Chen WL, Striz AG, Bert CW. High accuracy plane stress and plate element in the quadrature element method. Int J Solids Struct 2000;37:627–47.
[124] Shu C. An efficient approach for free vibration analysis of conical shells. Int J Mech Sci 1996;38(8–9):935–49.
[125] Shu C. Free vibration analysis of composite laminated conical shells by generalized differential quadrature. J Sound Vib 1996;194:587–604.
[126] Shu C, Du H. Free vibration analysis of composites cylindrical shells by DQM. Compos Part B Eng 1997;28:267–74.
[127] Viola E, Tornabene F. Vibration analysis of conical shell structures using GDQ method. Far East J Appl Math 2006;25:23–39.
[128] Tornabene F, Modellazione e Soluzione di Strutture a Guscio in Materiale Anisotropo [PhD thesis]. University of Bologna; 2007.
[129] Tornabene F, Viola E. Vibration analysis of spherical structural elements using the GDQ method. Comput Math Appl 2007;53:1538–60.
[130] Zong Z, Zhang YY. Advanced differential quadrature methods. CRC Press; 2009.
[131] Viola E, Tornabene F. Vibration analysis of damaged circular arches with varying cross-section. Struct Integr Durab (SID-SDHM) 2005;1:155–69.
[132] Viola E, Dilena M, Tornabene F. Analytical and numerical results for vibration analysis of multi-stepped and multi-damaged circular arches. J Sound Vib 2007;299:143–63.
[133] Marzani A, Tornabene F, Viola E. Nonconservative stability problems via generalized differential quadrature method. J Sound Vib 2008;315:176–96.
[134] Tornabene F, Viola E. 2-D solution for free vibrations of parabolic shells using generalized differential quadrature method. Eur J Mech A Solid 2008;27: 1001–25.
[135] Tornabene F, Marzani A, Viola E, Elishakoff I. Critical flow speeds of pipes conveying fluid by the generalized differential quadrature method. Adv Theor Appl Mech 2010;3:121–38.
[136] Tornabene F. 2-D GDQ solution for free vibrations of anisotropic doubly-curved shells and panels of revolution. Compos Struct 2011;93:1854–76.
[137] Tornabene F. Free vibrations of anisotropic doubly-curved shells and panels of revolution with a free-form meridian resting on Winkler–Pasternak elastic foundations. Compos Struct 2011;94:186–206.
[138] Tornabene F, Liverani A, Caligiana G. Laminated composite rectangular and annular plates: a GDQ solution for static analysis with a posteriori shear and normal stress recovery. Compos Part B Eng 2012;43:1847–72.
[139] Tornabene F, Liverani A, Caligiana G. Static analysis of laminated composite curved shells and panels of revolution with a posteriori shear and normal stress recovery using generalized differential quadrature method. Int J Mech Sci 2012;61:71–87.
[140] Tornabene F, Liverani A, Caligiana G. General anisotropic doubly-curved shell theory: a differential quadrature solution for free vibrations of shells and panels of revolution with a free-form meridian. J Sound Vib 2012;331: 4848–69.
[141] Bayat M, Aghdam MM. A micromechanics based analysis of hollow fiber composites using DQEM. Compos Part B Eng 2012;43:2921–9.
[142] Fantuzzi N, Generalized differential quadrature finite element method applied to advanced structural mechanics [PhD thesis]. University of Bologna; 2013.
[143] Ferreira AJM, Viola E, Tornabene F, Fantuzzi N, Zenkour AM. Analysis of sandwich plates by generalized differential quadrature method. Math Prob Eng 2013;2013:1–22. Article ID 964367.
[144] Tornabene F, Ceruti A. Free-form laminated doubly-curved shells and panels of revolution resting on Winkler–Pasternak elastic foundations: a 2-D GDQ solution for static and free vibration analysis. World J Mech 2013;3:1–25.
[145] Tornabene F, Fantuzzi N, Viola E, Ferreira AJM. Radial Basis Function method applied to doubly-curved laminated composite shells and panels with a general higher-order equivalent single layer theory. Compos Part B Eng 2013;55:642–59.
[146] Tornabene F, Reddy JN. FGM and laminated doubly-curved and degenerate shells resting on nonlinear elastic foundations: a GDQ solution for static analysis with a posteriori stress and strain recovery. J Indian Inst Sci 2013;93:635–88.
[147] Tornabene F, Viola E. Static analysis of functionally graded doubly-curved shells and panels of revolution. Meccanica 2013;48:901–30.

[148] Tornabene F, Viola E, Fantuzzi N. General higher-order equivalent single layer theory for free vibrations of doubly-curved laminated composite shells and panels. Compos Struct 2013;104:94–117.
[149] Viola E, Tornabene F, Fantuzzi N. General higher-order shear deformation theories for the free vibration analysis of completely doubly-curved laminated shells and panels. Compos Struct 2013;95:639–66.
[150] Viola E, Tornabene F, Fantuzzi N. Static analysis of completely doubly-curved laminated shells and panels using general higher-order shear deformation theories. Compos Struct 2013;101:59–93.
[151] Mosallaie Barzoki AA, Ghorbanpour Arani A, Kolahchi R, Mozdianfard MR, Loghman A. Nonlinear buckling response of embedded piezoelectric cylindrical shell reinforced with BNNT under electro-thermo-mechanical loadings using HDQM. Compos Part B Eng 2013;44:722–7.
[152] Viola E, Tornabene F, Fantuzzi N. Generalized differential quadrature finite element method for cracked composite structures of arbitrary shape. Compos Struct 2013;106:815–34.
[153] Viola E, Tornabene F, Ferretti E, Fantuzzi N. Soft core plane state structures under static loads using GDQFEM and cell method. CMES 2013;94:301–29.
[154] Viola E, Tornabene F, Ferretti E, Fantuzzi N. GDQFEM numerical simulations of continuous media with cracks and discontinuities. CMES 2013;94:331–68.
[155] Viola E, Tornabene F, Ferretti E, Fantuzzi N. On static analysis of plane state structures via GDQFEM and cell method. CMES 2013;94:419–56.
[156] Fantuzzi N, Tornabene F. Strong formulation finite element method for arbitrarily shaped laminated plates – I. theoretical analysis. Adv Aircr Space Sci 2014;1:124–42.
[157] Fantuzzi N, Tornabene F. Strong formulation finite element method for arbitrarily shaped laminated plates – II. numerical analysis. Adv Aircr Space Sci 2014;1:143–73.
[158] Fantuzzi N, Tornabene F, Viola E. Generalized differential quadrature finite element method for vibration analysis of arbitrarily shaped membranes. Int J Mech Sci 2014;79:216–51.
[159] Ferreira AJM, Carrera E, Cinefra M, Viola E, Tornabene F, Fantuzzi N, et al. Analysis of thick isotropic and cross-ply laminated plates by generalized differential quadrature method and a unified formulation. Compos Part B Eng 2014;58:544–52.
[160] Tornabene F, Fantuzzi N, Viola E, Carrera E. Static analysis of doubly-curved anisotropic shells and panels using CUF approach, differential geometry and differential quadrature method. Compos Struct 2014;107:675–97.
[161] Tornabene F, Fantuzzi N, Viola E, Reddy JN. Winkler–Pasternak foundation effect on the static and dynamic analyses of laminated doubly-curved and degenerate shells and panels. Compos Part B Eng 2014;57:269–96.
[162] Tornabene F. Free vibrations of laminated composite doubly-curved shells and panels of revolution via the GDQ method. Comput Methods Appl Mech Eng 2011;200:931–52.
[163] Wang X, Wang X, Shi X. Accurate buckling loads of thin rectangular plates under parabolic edge compressions by the differential quadrature method. Int J Mech Sci 2007;49:447–53.
[164] Viola E, Tornabene F, Fantuzzi N, DiQuMASPAB software, DICAM department, Alma mater studiorum – University of Bologna; 2013, <http://software.dicam.unibo.it/diqumaspab-project>.
[165] Pagano NJ. Exact solutions for rectangular bidirectional composites and sandwich plates. J Compos Mater 1970;4:20–34.
[166] Noor AK, Burton WS, Peters JM. Predictor–corrector procedures for stress and free vibration analyses of multilayered composite plates and shells. Comput Methods Appl Mech Eng 1990;82:477–95.
[167] Malik M, Noor AK. Accurate determination of transverse normal stresses in hybrid panels subjected to electro-thermo-mechanical loadings. Int J Numer Methods Eng 2000;47:477–95.
[168] Chaudhuri RA, Seide P. An approximate semi-analytical method for prediction of interlaminar shear stresses in an arbitrarily laminated thick plate. Compos Struct 1987;25:627–36.
[169] Zhang GM, Batra RC. Modified smoothed particle hydrodynamics method and its application to transient problems. Comput Mech 2004;34:137–46.
[170] Zhang GM, Batra RC. Symmetric smoothed particle hydrodynamics (SSPH) method and its applications to elastic problems. Comput Mech 2009;43:321–40.
[171] Zhang GM, Batra RC. Wave propagation in functionally graded materials by modified smoothed particle hydrodynamics (MSPH) method. J Comput Phys 2007;222:374–90.